DART: Automatic Blade Pitch & Performance Optimization for Propeller-Driven Aircraft and UAVs

Franklín Andrésson Chief of Development, **TERRN**.DYNAMICS

> Version 1.2 Published March 14th, 2025.

Sponsored by SimScale, Providing Digital Aerodynamic Simulations

Table of Contents

Table of Contents	1
1. Abstract	3
2. Figures & Definitions	4
2.1 Aerodynamics	4
2.2 Aviation	6
2.3 Mechanisms & Hardware	8
2.4 Mathematics & Programming	9
2.5 List of Figures	10
3. Introduction	12
3.1 Problem Statement	12
3.2 Project Objectives	13
3.3 Significance of Research	13
3.4 Overview of Paper	14
3.5 Risk Assessment	14
4. Background	16
4.1 State of the Art	_
4.1.1 Constant-Speed Propellers	16
4.1.2 Variable & Fixed-Pitch Propellers	17
4.1.3 Aircraft Sensors & Data	17
4.1.4 Electric Propulsion in Aviation	
4.1.5 P-factor Mitigation & Control	18
4.2 Key Principles	19
4.2.1 Efficiency Through Active Angle-of-Attack Control	
4.2.2 Adaptive Propeller Pitch Control	19
4.2.3 Real-Time Performance Computation	20
4.2.4 P-factor Mitigation & Leveraging	20
5. Prototyping Process & Methodology	21
5.1 Prototype Overview	21
5.2 Actuator Design	23
5.2.1 ARC M1 Systems & Electronics Overview	
5.3 Prototype Hardware Design	29
5.4 Prototype Software Design	30
5.4.1 Method for Modeling Optimal Alpha	31
5.4.2 Method for Modeling High-Thrust Alpha	35
5.4.3 Method for Modeling Reverse-Thrust Alpha	37
5.4.4 Phase-of-Flight (PoF)	39
5.4.5 Digital Pitch Control System (DPCS)	
5.4.6 P-factor Augmentation & Control Enhancement (PACE)	
5.5 Technical Software Implementation	
5.5.1 Input Data Control	
5.5.2 Systems Integration	
6. Results	48

6.1 Preliminary Prototype Performance	48
6.2 Digital Wind Tunnel Performance	49
6.2.1 Mathematically Governed Thrust Performance Data	50
6.2.2 Revised Thrust Performance Data	51
6.2.3 Turbulent Kinetic Energy Represented Airflow	52
6.2.4 Velocity Represented Airflow	54
6.2.5 Low-Pressure Represented Volumes	55
6.2.6 PACE System Performance	56
7. Discussion	57
7.1 Key Results	57
7.2 Overall Performance Evaluation	58
7.3 Aerodynamic Analysis	59
7.4 Operational & Systems Integration	61
7.5 Feasibility & Safety	62
7.6 Broader Implications & Significance	62
7.7 Future Work & Improvements	
8. Conclusion	64
9. References	65

1. Abstract

The efficiency of propeller-driven aircraft is heavily dependent on propeller pitch control. Traditional propeller systems such as fixed-pitch propellers offer limited efficiency throughout the various conditions and phases of flight an aircraft may encounter. Even with more sophisticated systems such as constant-speed propellers, the aim is to maintain a set rotational speed of the engine, adjusting the propeller blades in order to regulate it. This highlights a gap in technology for a new generation of alternative-fuel aircraft such as ones driven by electricity where the motors can operate efficiently across a wide range of speeds, allowing for the implementation of a system that focuses on the aerodynamic utilization and efficiency of the propeller blade.

To advance innovation and to further improve propeller-driven aircraft and UAV efficiency, this research paper presents the Digital Airflow-Reactive Tuning, or DART, system, along with its entire development process, from conceptualization, physical realization, through to computational fluid dynamics testing.

Through results by computational fluid dynamics simulations, DART is proven to reduce the torque-resistive aerodynamic drag of the propeller blade by as **much as 60**% depending on its configuration and operational requirements compared to a cruise-optimized fixed-pitch propeller in a takeoff scenario without large penalties in thrust output. The **increase in thrust-to-torque-resistive-drag** ratio was evident throughout the computational fluid dynamics simulation runs, to varying degrees based on the scenario the system was tested in.

DART utilizes existing technology and leverages systems already found on modern aircraft, decreasing the initial costs of its implementation and enhancing its feasibility. While targeting the aerodynamic efficiency of propeller blades, namely the reduction in drag counteracting the propeller's rotation, DART introduces an array of improvements upon current propeller technology that enhance overall and operational efficiency through the implementation of its various subsystems such as PoF (Phase-of-Flight), which can automatically determine the phase of flight and current desired performance characteristics of the aircraft, eliminating manual pitch control along with the risk of human operator error.

In summary, DART demonstrates **significant performance enhancements**, particularly in fixed-pitch propeller systems, laying the foundation for advancing efficient electric propeller propulsion technology. With potential applications in light aircraft and UAVs, DART offers multi-faceted advantages **extending beyond just aircraft performance**, **contributing to more sustainable aviation operations**.

2. Figures & Definitions

2.1 Aerodynamics

- Angle of Attack: Describes the angle between the *chord line* and *relative airflow* going over the wing. It can be referred to as α or alpha.
- **Airfoil:** A specific shape designed to exercise specific aerodynamic characteristics such as high lift or low drag. Can be referred to as a **wing profile**.
- **Chord Line:** An imaginary line drawn from the *leading edge* to the *trailing edge* of an *airfoil*.
- Leading Edge: The point of the airfoil that hits the airflow first.
- **Trailing Edge:** Opposite of the *leading edge*, being the last point of contact between the airflow and *airfoil*.
- **P-factor:** An often undesired *yawing* moment of the aircraft due to asymmetric thrust generation. Resulting yawing tendencies are often found on single-engine propeller aircraft when they are taking off.
- Yaw: Rotation around the aircraft's vertical axis.
- **Pitch:** Rotation around the aircraft's *lateral axis* that extends across the wings.
- **Roll:** Rotation around the aircraft's *longitudinal axis* that extends along its length.
- **Lift:** The aerodynamic force that pulls the wing upwards, or if rotated 90°, can produce **thrust** for a propeller aircraft.
- **Drag:** The aerodynamic force that tries to counteract the forward movement of an *airfoil* or object through air.
- **Lift Coefficient:** Often referred to as **C**_L, it is a dimensionless quantity often used to calculate the *lift* generated by a wing with a certain *airfoil*.
- Drag Coefficient: Often referred to as C_D, it is a dimensionless quantity often used in calculating the drag generated by a wing with a certain airfoil.
- **Reynolds Number:** Often referred to as **Re**, it is a dimensionless quantity that indicates how turbulent or laminar a certain air or fluid flow is.
- **Relative Airflow:** The *resultant vector* created by an object's movement through air combined with any external airflow, such as winds.
- Laminar Airflow: A flow of fluid, gas or liquid, that is smooth and flows in regular paths.

- **Turbulent Airflow:** A flow of fluid, gas or liquid, that is rough and flows in irregular paths.
- **Stall:** An aerodynamic phenomenon associated with the loss of lift. When an *airfoil* experiences too high of an angle-of-attack, the airflow becomes turbulent and results in the low-pressure zone over the airfoil deteriorating, significantly decreasing lifting forces.
- **Torque-Resistive Drag:** A form aerodynamic drag that resists the continuous rotation of the propeller. The reduction of it can reduce the energy needed to keep a rotating object in motion.
- Turbulent Kinetic Energy: The mean kinetic energy per mass associated with eddies
 in turbulent flow. The presence of turbulent kinetic energy, or TKE, indicates turbulent
 flow in a given airstream, sometimes resulting in aerodynamic inefficiencies as seen
 in this report.
- **Computational Fluid Dynamics:** The process of using computer simulations, often referred to as **CFD**, to model the flow of a fluid, often around or within a defined geometry, to gain insights into its interaction with the given fluid flow.

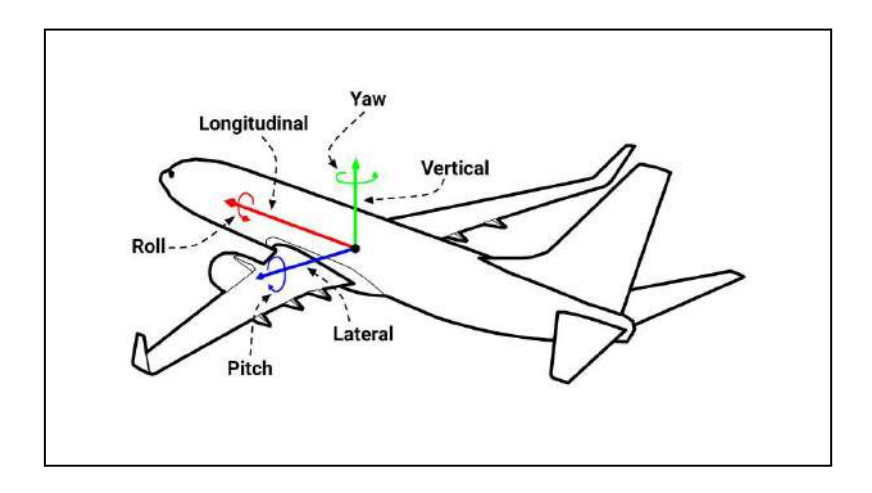


Fig. 2.1A, Axes of Aircraft Rotation

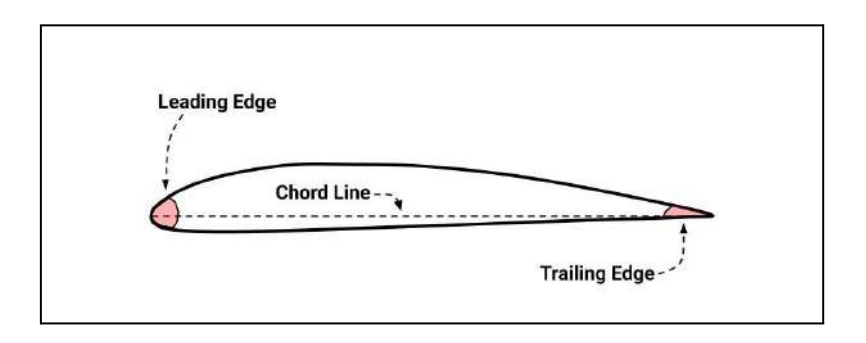


Fig. 2.1B, Airfoil Diagram

2.2 Aviation

- Airspeed: The speed of the aircraft relative to the air moving around it.
- IAS: Indicated airspeed is derived from the *dynamic pressure* read by the *pitot tube*.
- **TAS:** True airspeed is derived from the *dynamic pressure* read by the *pitot tube* and where atmospheric factors such as *static pressure* and temperature are compensated for.
- **ASL:** Altitude above sea level, the standard for conveying aircraft altitude.
- AGL: Altitude above ground level, used to convey altitude above the ground.
- **RPM:** Revolutions per minute, used to label rotational speed.
- **Ground Speed:** The speed of the aircraft relative to the ground beneath it.
- Maneuvering Area: Airport surfaces aircraft use for taxiing, taking off, and landing.
- **Taxiway:** Surface of an airport that aircraft use for **taxiing**. Their primary use is to enable movement between *terminals* and *runways*.
- **Runway:** Surface of an airport that aircraft use to perform *take-offs* and *landings*. This surface is characterized by aircraft at high speeds and stringent safety protocols.
- **Propeller Pitch:** How far the propeller would move forward in one rotation if it was moving through a solid, much like screws going into wood.
- Blade Angle: Specifies the angle between the blade's chord line and its plane of rotation, directly related to propeller pitch but specifies an angle instead of linear movement.
- **Aircraft Rotation**: Refers to the aircraft pointing its nose upwards and lifting off the ground.
- **Takeoff Phase:** The part of an aircraft's flight that is characterized by a very high thrust setting and intent of accelerating the aircraft to an airspeed at which it can generate enough lift to overcome the gravitational force and subsequent flight.
- **Climb Phase:** The part of an aircraft's flight that is characterized by a slightly lower *thrust setting* with the primary goal of increasing the aircraft's altitude while accelerating slowly.
- **Cruising Phase:** The part of an aircraft's flight that is characterized by a high yet stable altitude and high speed.
- **Descent Phase:** The part of an aircraft's flight that is characterized by the intent of decreasing the aircraft's altitude in preparation for landing.
- **Approach Phase:** The part of an aircraft's flight that is characterized by a low altitude and low speeds with the primary goal being to navigate to a specific runway.

- Landing Phase: The part of an aircraft's flight that is characterized by even lower altitudes and low speeds where the aircraft gets close to the ground and eventually touches down on a runway. A thrust reversal and braking usually follow this to decelerate the aircraft.
- Reverse Thrust: Used to alleviate the brakes of excessive wear and tear during landing. This reversal of airflow is achieved through various means depending on the type of engine used.
- **Go-Around:** A procedure, following an *aborted landing*, where the aircraft accelerates and climbs to a safer altitude to try landing again later.
- **UAV:** An Unmanned Aerial Vehicle, could also be known as a drone.
- **Feathering:** A procedure where the blades of a propeller are angled in such a manner as to provide the least aerodynamic resistance to an aircraft moving forward in flight, often performed due to an engine failure.

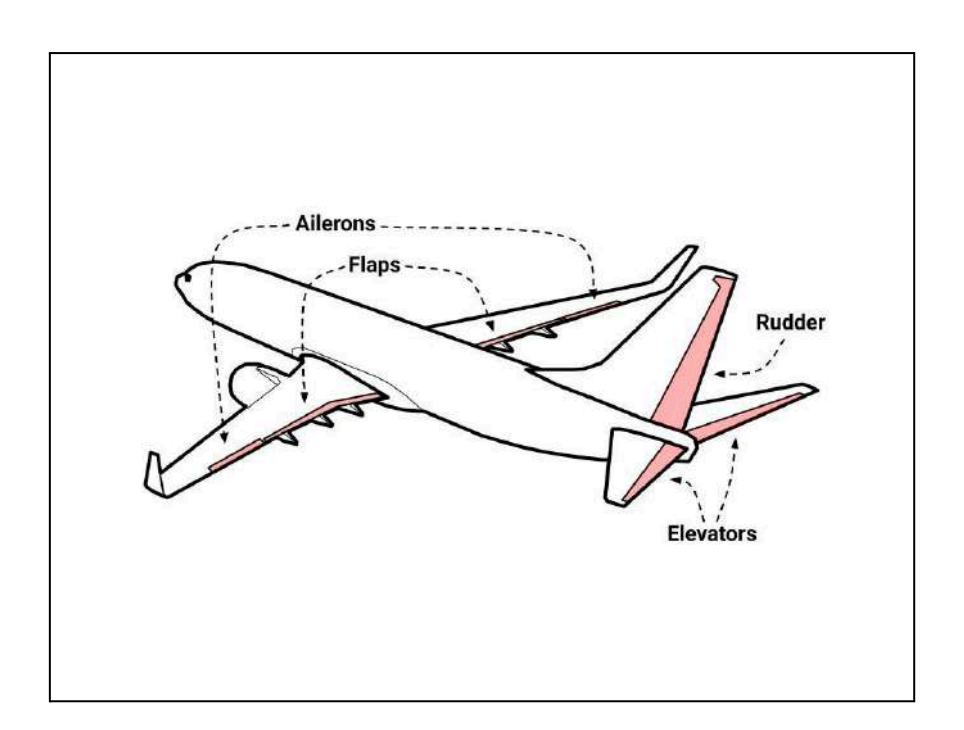


Fig. 2.2A, Aircraft Control Surfaces

2.3 Mechanisms & Hardware

- Swashplate Mechanism: Commonly found on helicopters due to enabling rotor blade control while in motion. Two primary control functions are the *collective*, which controls the blade angles simultaneously augmenting overall lift, and *cyclic*, which can vary the blade angles throughout their rotation, essentially tilting the lift in a certain direction.
- **Collective Pitch:** As stated above, collective pitch refers to the collective and equal manipulation of all propeller blades.
- **Cyclic Pitch:** As stated above, cyclic pitch refers to a pitch difference experienced by the propeller blades throughout their rotation or cycle, useful for generating asymmetric thrust.
- **Propeller Disc:** The circular area of which the propeller blades occupy during their rotation.
- Constant-Speed Propeller: Widely used in more advanced propeller-driven aircraft. They use aerodynamic forces acting on the propeller blades in order to keep the engine at a set rotational speed to achieve optimal performance and efficiency.
- **Fixed-Pitch Propeller:** Widely used in light and simpler aircraft where the propeller blades are not able to be adjusted and are designed to be efficient at a certain speed and rotational speed.
- Variable-Pitch Propeller: Common in more advanced light aircraft where you are able to adjust the blade angle throughout the flight to achieve desired performance and efficiency in certain phases of the flight.
- **Turboprop:** A type of engine that uses a smaller jet engine to drive a propeller via a turbine. These are commonly found on short-haul regional aircraft.
- Rudder: A control surface that enables aircraft rotation around its vertical axis.
- **Elevator:** A control surface that enables aircraft rotation around its lateral axis.
- Aileron: A control surface that enables aircraft rotation around its longitudinal axis.
- **Flaps:** A control surface on a wing's trailing edge that increases wing area and angle of attack, allowing for slower flight.
- **Actuator:** A form of motion control technology that comes in many forms, such as rotary or linear, depending on their end-use case.

2.4 Mathematics & Programming

- Regression: In the case of this paper, individual points of data are used to produce a
 function, enabling estimation and calculation of inputs outside of or between data
 points.
- **Coefficient of Determination:** Used to gauge how accurately a regression reflects the individual data points.
- Python: A popular programming language that is heavily used in the systems of DART.
- **PWM:** Pulse Width Modulation is a popular method of communicating values between, for example, a computer and an actuator through varying the length of a pulse in proportion to a set frequency.
- Closed-Loop System: A system that receives continuous feedback allowing detection and correction of errors, enabling precise outputs.
- Homing Sequence: Common for non-closed loop systems, a homing sequence is used to determine where an end-effector, such as what position an actuator, is by moving it until it reaches a known point.

2.5 List of Figures

- Fig. 2.1A Axes of Aircraft Rotation, Created by author, 2025
- Fig. 2.1B Airfoil Diagram, Created by author, 2025
- Fig. 2.2A Aircraft Control Surfaces, Created by author, 2025
- Fig. 4.1.1A Bombardier Dash-8 Q400 & Q200, Photographed by author, 2023
- Fig. 4.1.1B ATR 72-600, Photographed by author, 2023
- **Fig. 4.2.4A** The Author landing a Single-Engine Cessna 172N Skyhawk, Photographed by Flight Instructor, 2024
- **Fig. 5.1A** Bo105 Rotorkopf, Bernd vdB, CC-BY-SA-2.5 https://commons.wikimedia.org/wiki/File:Bo105_Rotorkopf_0570b.jpg
- Fig. 5.2B Photo of DART Prototype, Photographed by author, 2025
- Fig. 5.2A ARC M1 SMD Technical Drawing & Overview, Created by author, 2025
- Fig. 5.2B ARC M1 Technical Drawing Externals & Internals, Created by author, 2025
- Fig. 5.2C ARC M1 Mounted on the DART Prototype, Photographed by author, 2025
- Fig. 5.2.1A ARC M1 Systems & Components Overview, Created by author, 2025
- Fig. 5.2.1B Motherboard Components, Created by author, 2025
- Fig. 5.2.1C PDB & Motherboard, Created by author, 2025
- Fig. 5.2.1D ARC M1 Motherboard Schematic, Created by author, 2025
- Fig. 5.4A DART Subsystems Overview & Processes, Created by author, 2025
- Fig. 5.4.1A Cubic Regression of Clark-Y C_L v Alpha, Re = 50.000, $R^2 \approx 0,994$, Created by author, 2025
- **Fig. 5.4.1B** Quadratic Regression of Clark-Y C_D v Alpha, Re = 50.000, $R^2 \approx 0,769$, Created by author, 2025
- Fig. 5.4.1C Clark-Y C_L v Alpha at varying Re, Created by author, 2025
- Fig. 5.4.1D Clark-Y C_L/C_D v Alpha, Re = 50.000, Created by author, 2025
- Fig. 5.4.1E Exponential Regression of Clark Y Optimal Alpha v Re, $R^2 \approx 0,922$, Created by author, 2025
- Fig. 5.4.2A Clark-Y C_L v Alpha with stall zones illustrated, Created by author, 2025
- Fig. 5.4.2B Clark-Y C_L v Alpha with C_L Maximum restrictions, Created by author, 2025

- **Fig. 5.4.2C** Linear Regression of Clark Y High-Thrust Alpha v Re, $R^2 \approx 0.786$, Created by author, 2025
- Fig. 5.4.3A Clark-Y C_L v Alpha with C_L Minimum restrictions, Created by author, 2025
- Fig. 5.4.3B Linear Regression of Clark Y Reverse Thrust Alpha v Re, $R^2 \approx 0.854$, Created by author, 2025
- Fig. 5.4.5A DPCS Reynolds Number Computation Process, Created by author, 2025
- Fig. 5.4.5B DPCS True Airspeed Computation Process, Created by author, 2025
- Fig. 5.4.5C DPCS Airflow Vector Computation Process, Created by author, 2025
- Fig. 5.5.1A Upper Portion of DART MDII, Created by author, 2025
- Fig. 5.5.2A Lower Portion of DART MDII Showing Python Lists, Created by author, 2025
- Fig. 5.5.2B Technical Python Program Layout of DART, Created by author, 2025
- Fig. 6.2A General Performance Comparison Overview, Created by author, 2025
- **Fig. 6.2.1A** Mathematically-Governed DART Performance v Fixed-Pitch Table, Created by author, 2025
- **Fig. 6.2.1B** Mathematically-Governed DART Performance v Fixed-Pitch Graph, Created by author, 2025
- Fig. 6.2.2A Revised DART Performance v Fixed-Pitch Table, Created by author, 2025
- Fig. 6.2.2B Revised Takeoff-Oriented DART Pitch v Fixed-Pitch, Created by author, 2025
- Fig. 6.2.2C Revised Climb-Oriented DART Pitch v Fixed-Pitch, Created by author, 2025
- **Fig. 6.2.3A** TKE-Colored Airflow Analysis of the Cruise-Optimized Fixed-Pitch Propeller, Created by author, 2025
- **Fig. 6.2.3B** TKE-Colored Airflow Analysis of the Cruise-Optimized Fixed-Pitch Propeller, Created by author, 2025
- **Fig. 6.2.3C** TKE-Colored Airflow Analysis of the DART Controlled 25 α Propeller, Created by author, 2025
- Fig. 6.2.3D TKE-Colored Airflow Analysis of the DART Controlled 25 α Propeller, Created by author, 2025
- **Fig. 6.2.4A** Velocity-Colored Airflow Analysis of the Cruise-Optimized Fixed-Pitch Propeller, Created by author, 2025
- **Fig. 6.2.4B** Velocity-Colored Airflow Analysis of the DART Controlled 25 α Propeller, Created by author, 2025

- **Fig. 6.2.5A** Pressure-Colored Volume Analysis of the Cruise-Optimized Fixed-Pitch Propeller, Created by author, 2025
- Fig. 6.2.5B Pressure-Colored Volume Analysis of the DART Controlled 25 α Propeller, Created by author, 2025
- Fig. 6.2.6A Non-PACE Adjusted DART Propeller, Created by author, 2025
- Fig. 6.2.6B PACE Adjusted DART Propeller, Created by author, 2025
- **Fig. 7.3A** Noted TKE-Colored Airflow Analysis of the DART Controlled 25 α Propeller, Created by author, 2025
- **Fig. 7.3B** Noted TKE-Colored Airflow Analysis of the Cruise-Optimized Fixed-Pitch Propeller, Created by author, 2025
- **Fig. 7.3C** Noted Velocity-Colored Airflow Analysis of the Cruise-Optimized Fixed-Pitch Propeller, Created by author, 2025
- **Fig. 7.3D** Noted Pressure-Colored Volume Analysis of the Cruise-Optimized Fixed-Pitch Propeller, Created by author, 2025

3. Introduction

This section outlines the DART project which seeks to optimize propeller-driven propulsion technology through real-time advanced digital systems. The challenges DART aims to address and the potential significance of this research are also highlighted, alongside a brief overview of the paper.

3.1 Problem Statement

With the advent of new technologies within the aviation industry, challenges arise in effectively integrating these innovations into our existing systems. As the demand for efficient and versatile aircraft rises, particularly in the UAV sector, solutions must address operational efficiency and sustainability. Simultaneously, heightened awareness of our climate has put overall efficiency and the lowering of emissions at the forefront of innovation, further accentuating the demand for integrating these advanced systems for optimization in both the creation and operation of our aircraft, regardless of size.

- In modern constant-speed systems, the propeller's RPM is regulated through propeller pitching, that is, changing the angle at which the air hits the propeller blades ("Constant Speed Propeller", n.d.). This is crucial to keep the engine running within its narrow band of efficient RPMs. However, UAVs and several up-and-coming aircraft are being fitted with electric motors with a much wider range of efficient RPMs (biswayandutta2000, 2024), creating a gap where systems that can simultaneously accommodate an efficient RPM and an aerodynamically efficient propeller blade angle are still in the research and development phase.
- Furthermore, in less sophisticated systems such as variable-pitch propellers, any kind of real-time adjustment of the propeller pitch is absent, requiring manual pilot inputs ("Variable Speed Propeller", n.d.). These limitations are even more apparent in fixed-pitch propeller systems where you are not able to adjust the propeller pitch at all. This presents an array of issues regarding not only overall efficiency but also aircraft performance throughout a flight.
- Finally, aside from the surface-level propeller pitch issues, challenges arise in how we handle the aerodynamic phenomena known as p-factor. When single-engine propeller aircraft are at high angle-of-attacks, such as when they perform their initial rotation off of the runway, this phenomenon results in a yawing moment that tries to turn the aircraft either left or right depending on the propeller's direction of rotation. This is often mitigated through control surface deflections manually performed by pilots and results in a predictable and expected yawing motion still needing to be manually accounted for and corrected, presenting slight maneuverability difficulties.

3.2 Project Objectives

The problems listed above apply to both current and future aerial vehicles, to varying degrees, and serve as the guide rails for what challenges DART aims to address. The main focus of this project and research is to both increase overall and operational efficiency, with the lowering of emissions and assisting the effective integration of electric propulsion being derivatives of them.

- For propeller-driven aircraft, with electricity as their main propulsion in particular, this project aims to replace the systems that rely on mechanical feedback to the governor from the propeller blades found in constant-speed systems with the processing of digital sensor signals to accurately model the airflow over each propeller blade in real-time, allowing for adaptive propeller pitching that ensures a suitable angle-of-attack experienced by each propeller blade, increasing their aerodynamic efficiency.
- In addition, there is a goal to implement a system that reads flight data and control
 parameters to determine what phase of flight the aircraft is situated in, eliminating
 the need for any manual propeller pitch adjustment found in both constant-speed
 and variable-pitch propeller systems, potentially increasing both overall efficiency and
 performance throughout the various phases of flight.
- Lastly, the implementation of a new type of propeller control system is also to be done. Such a system aims to not only mitigate p-factor effects in real-time but also harness the aerodynamic phenomena in a way to assist in the maneuvering of smaller UAVs operating in rough conditions. This type of asymmetrical thrust generation is common in helicopter rotor systems.

3.3 Significance of Research

The significance of the research, both from a technological standpoint and its potential contributions to our collective efforts to reduce our atmospheric impact, has the possibility of laying out the groundwork for future research and developments through the various systems previously mentioned in the project's objectives. DART aims to improve our propeller technology for both current and future aircraft, a goal that can prove useful due to the significant expected increase in the UAV market within the coming years ("Unmanned Aerial Vehicle (UAV) Drones Market Size Expected to Reach USD 169.7 Bn by 2033", 2024).

Moreover, data suggests a sizeable reduction in our climate impact through the use of medium-range climate-optimal turboprop aircraft (Thijssen et al., 2022). Implementing certain aforementioned systems could benefit such propeller-driven aircraft and align with our global initiatives due to potentially increased overall aircraft efficiency.

In conclusion, the means by which DART aims to address current and future issues, specifically through its use of both hardware and software that are oriented to both improve the aerodynamic efficiency of propeller-driven, especially electrically powered, aircraft and

the potential operational efficiency tied to leveraging p-factor in UAV maneuvering, could prove useful from a multitude of perspectives.

3.4 Overview of Paper

This paper serves as a summary of the research and the process by which results were interpreted and established. The aim is to not only define the DART project, namely that of its potential impacts in various fields, but to also give insight into how this project came to be and how it underwent continuous development until it became what it is today.

The paper starts with an introduction followed by a background section, providing clear answers to what issues DART aims to address and by which means they are solved. A look back at our current technology and a deeper dive into its gaps is also present. The prototyping and methodology section documents the design and construction of the hardware and software in this project, subjects such as outlining, revising, and component manufacturing methods are also discussed here. This section is rounded off with system architecture and implementation, describing how the digital systems are merged with mechanical ones, both in the prototype itself and in hypothetical aircraft. Results and the discussion sections follow suit and present the findings from a digital wind tunnel analysis and the performance of the DART prototype. Discussions regarding the implementation of the DART system in aircraft and potential future adjustments are held in combination with analyzing the results.

Lastly, the conclusion section summarizes the findings and discussions, providing an overview of what DART has achieved and what conclusions can be drawn from its development and results. A reference list can also be found afterward.

3.5 Risk Assessment

There are minor risks regarding this project associated with personal injury. The tools used can impose risks and injury if not handled correctly, as with most equipment. However, below is a list of the equipment which pose a more defined risk to injury and health, as opposed to general risks associated with the incorrect handling of any equipment.

- Soldering Iron: This is used to assemble the circuit boards and miscellaneous permanent electrical connections through melting, most commonly, a mix of lead and tin. It is advisable not to breathe in the fumes, hence why this project utilized lead-free soldering tin. Alongside the fumes, there is the hot soldering iron that often reaches temperatures above 300°C, presenting severe burn risks if the user does not delegate proper care and handling. The risks were mitigated through the careful and proper use of the equipment.
- Fused-Deposition Modeling 3D-Printer: The practice of melting plastics does come
 with the generation of fumes. Nanoparticles and VOC's (Volatile Organic Carbon)
 have been found to be emitted from 3D-printers during their operation, presenting a
 health risk if inhaled, especially for longer periods of time. This is combined with the
 risk of burns when changing the nozzle of the printer if the nozzle hasn't cooled

down. The aforementioned risks are reduced through opening the window of the room the printer is operating in, increasing ventilation, and making sure through the printer's interface that the nozzle is not too hot to touch and handle.

4. Background

The background section aims to provide the reader with the knowledge needed to understand the situation we are currently in and how it has evolved alongside an overview of what principles DART adheres to.

4.1 State of the Art

This section outlines what technology and methods we utilize today and how they function. This is crucial to understand what DART is aiming to build upon and replace while also getting insight into the current technological situation. Our current engine and propeller technologies and sensors are mentioned, with an overview of the use of electric propulsion in smaller aerial vehicles and how P-factor is handled.

4.1.1 Constant-Speed Propellers

The mission of a constant-speed propeller system is, as its name suggests, to maintain a constant rotational speed. The pilot selects a desired RPM and a governor mechanism automatically maintains it through the use of propeller pitching ("Constant Speed Propeller", n.d.) As the angle of attack of the propeller blades increases, so does their drag, creating a force that resists the propeller's rotation and slows down the engine. Conversely, when the angle of attack of the propeller decreases, the load on the engine also decreases, increasing RPM. This pitch change is closed-loop and continuous, maintaining the set RPM regardless of any fluctuating external factors.

In summary, RPM is maintained through the continuous adjustment of the propeller pitch. This continuous pitch adjustment is crucial for efficiency in conventional fuel-driven aircraft. Modern commercial aircraft such as Bombardier's Dash-8 series and ATR's 72 series utilize systems like FADEC that replace the mechanical governor with a digital control system, enabling more precise adjustments to propeller pitch and engine parameters, further enhancing efficiency ("Full Authority Digital Engine Control (FADEC)", n.d.)



Fig. 4.1.1A, Bombardier Dash-8 Q400 & Q200



Fig. 4.1.1B, ATR 72-600

4.1.2 Variable & Fixed-Pitch Propellers

While not as advanced as a constant-speed propeller system, the variable-pitch propeller system still enables propeller pitch control, although without automatically maintaining an RPM. This system gives pilots manual control of the propeller pitch that can be utilized to tailor the aircraft's performance characteristics for each phase of the flight ("Variable Speed Propeller", n.d.).

Fixed-pitch propellers on the other hand, provide no control of the propeller pitch whatsoever, settling on a propeller blade that is designed to be functional in all phases of flight, with varying degrees of efficiency. However, they are popular in the general aviation sector due to their simplicity and reduced maintenance costs compared to more advanced systems ("Fixed Pitch Propeller", n.d.).

4.1.3 Aircraft Sensors & Data

On modern aircraft there is an array of sensors that provide crucial data to both the pilots and the flight computers. The DART system utilizes existing sensors found on commercial aircraft to enable its functions. Below is a brief breakdown of each relevant aircraft sensor alongside what their output data is:

- Pitot Tube: Essential to any winged aircraft, the pitot tube measures the dynamic pressure, that is, the pressure resulting from air moving into and being compressed in its tube. This pressure can then be used to calculate the speed of the air flowing around the aircraft, or as it is commonly referred to as, airspeed.
- Static Port: Another crucial sensor used to determine the altitude of the aircraft based on the static or atmospheric pressure around the aircraft. It is common to have to calibrate it by referencing the pressure at the departure or arrival airport.
- Angle of Attack Vane: Commonly found on commercial and more advanced general
 aviation aircraft, it is used to indicate the angle of the incoming air relative to a
 predetermined axis. The angle at which the air hits the wings, namely the angle of
 attack, is crucial in flight because it directly relates to the wing's performance.
- **RPM Sensor:** While the ways they function vary a lot between aircraft types and their operational requirements, these sensors are commonplace in aircraft today and are used to measure vital parameters such as the engine and propeller's RPM.
- **Gyroscope & IMU:** Similar to RPM sensors, the means by which the function and how they are utilized varies widely between aircraft, but they all share a common goal to provide the pilot and flight computers with the aircraft's orientation in three-dimensional space.
- Weight-on-Wheels: As its name suggests, this sensor that is found on more advanced aircraft is used to detect if there is a force being applied on the wheels, indicating that the aircraft is currently on the ground. This is often used to automatically perform control surface deflections and inhibit certain functions like reverse-thrust from being activated.

 Temperature Sensors: Very common in aviation and is used to measure ambient temperature in all sorts of systems. The data derived from them has many applications, such as indicating if any anti-ice systems need activation or to calculate TAS, or true airspeed.

The sensors mentioned all supply data to DART and its subsystems. Leveraging existing sensor technology is crucial for its mission, reducing both up-front and long-term costs associated with its implementation.

4.1.4 Electric Propulsion in Aviation

The context of which we will define electric propulsion within is the method of driving a propeller by an electric motor in order to generate thrust. Currently, large-scale propeller-driven aerial vehicles make use of combustion engines where the compression and expansion of gases exert a force that is translated into the rotational movement of a propeller. This is in stark contrast to electric motors that utilize magnetic fields to translate electrical energy into a rotational force, the means by which such translation of energy is achieved can vary between motor types. The use of electric motors brings with it a great increase in efficiency as outlined in CER's market snapshot, suggesting that over 77% of the energy stored in a battery-electric vehicle translates into movement, compared to internal-combustion engine vehicles lying at efficiency percentages as low as 12%. ("Market Snapshot: Battery electric vehicles are far more fuel efficient than vehicles with internal combustion engines", 2021).

The application of electric propulsion in the aviation industry today is mainly within the boundaries of small drones and fixed-wing UAVs. These boundaries are in large part set by the current limitations of our battery technologies, specifically regarding both energy density and cost. However, companies such as Eviation are already facilitating huge progress with their electric Alice aircraft, challenging the status quo and demonstrating the implementation of electric propulsion technology in large-scale manned aircraft.

4.1.5 P-factor Mitigation & Control

The current state of P-factor mitigation in fixed-wing aircraft lies in hardware design and control surface deflections. The specific methods for how p-factor is compensated for are aircraft specific. However, helicopters take full advantage of thrust asymmetry, generating it through the use of cyclic blade pitching to produce turning moments.

4.2 Key Principles

There are several key principles by which DART and its functions are governed by both its theoretical and practical implementation. These principles serve as the guide rails and ensure that DART fulfills its mission of automated, efficient, and safe propeller and aircraft control.

4.2.1 Efficiency Through Active Angle-of-Attack Control

The forces that an airfoil and resulting wing or propeller blade experience are a direct result of the angle at which the airflow is interacting with the airfoil relative to its chord line. The two primary forces are lift and drag, where the lift generates a force perpendicular to the airfoil's linear forward motion, while drag produces a force that is parallel to and opposes this motion. These two parameters are described in the form coefficients, namely C_L for the lift coefficient and C_D for the drag coefficient. Where efficiency is the greatest is where the most lift, or thrust in this case, is yielded for the least amount of drag. In contrast to the aircraft as a whole, the drag of the propeller blade primarily affects the torque necessary to rotate it, since drag would oppose the airfoil's forward rotational movement.

DART specifically targets the propeller blade's angle-of-attack in order to achieve desired performance characteristics, with them mainly being aerodynamic efficiency. The function of C_L and C_D for any given angle-of-attack is heavily dependent on a multitude of atmospheric and vector-related factors discussed later on. Therefore, DART continuously monitors such conditions and dynamically adjusts the propeller blades to the optimal angle-of-attack for the given mission without relying on manual pilot input. The efficiency gains stemming from the active control of propeller blade angle-of-attack would be the most pronounced in electrically-driven aircraft, as combustion engines in traditional aircraft often need to meet certain operational parameters in order to be efficient, often sacrificing the propeller's aerodynamic efficiency.

4.2.2 Adaptive Propeller Pitch Control

While overall efficiency is the primary goal of DART, operational efficiency is also paramount. This is the reason behind the usage of adaptive pitch control in the form of the Phase-of-Flight, or PoF, subsystem discussed in section 5.4.4. Over the course of an aircraft's flight, the desired performance characteristics and mission objectives change between its phases. When an aircraft reaches a safe altitude such as when it is in its climb, cruise, and descent phases, overall efficiency is in fact a priority. However, during critical phases such as takeoff, approach, and landing, quick accelerations and high control authority are crucial to retain a safe flight. Where large amounts of thrust are necessary, the angle-of-attack could be used to produce a large C_L , where overall lift and thrust is increased. This is often controlled manually in variable-pitch propeller systems, or disregarded completely in fixed-pitch propeller systems. However, DART aims to achieve automated control of the propeller pitch, reading various parameters and determining if efficiency or power is the current priority, optimizing the aircraft's performance for any given situation in real-time.

4.2.3 Real-Time Performance Computation

To achieve both effective control of the angle-of-attack and adaptive propeller pitching, a real-time system is utilized to accommodate the highly dynamic nature of aviation. DART would process sensor data that is already commonplace in modern aircraft and UAV's, such as airspeed, pressure, and temperature, to dynamically calculate the conditions of which the propeller blades are under and the forces acting upon them. This would in turn enable the aforementioned systems to function correctly.

4.2.4 P-factor Mitigation & Leveraging

The last principle by which DART aims to operate is through the mitigation and leveraging of thrust asymmetry, or as it's known more commonly in aviation, p-factor. This phenomena stems from the propeller's rotation and interaction with oncoming air, causing different sides of the propeller disc to generate different amounts of thrust and producing an often undesired yawing moment. This is often mitigated through manual pilot inputs and adds to maneuverability difficulties. These issues present themselves in single-engine propeller driven aircraft in particular.



Fig. 4.2.4A, The Author landing a Single-Engine Cessna 172N Skyhawk

However, the calculations necessary to anticipate p-factor are straight-forward vector mathematics, allowing DART to compensate for it in real time. There are also potential benefits to generate, not just compensate for, asymmetric thrust for smaller aircraft, such as UAVs in particular. When an aircraft is taking off and landing, it is "low and slow", meaning it doesn't have great speed or altitude, increasing the risk of an accident and making it vulnerable to adverse weather conditions. This is where a p-factor leveraging system could prove useful, providing crucial rudder control authority and like adaptive pitch, mitigating and leveraging p-factor increases not only operational efficiency, but also overall safety.

5. Prototyping Process & Methodology

This section describes the development of both the hardware and software that DART consists of. In addition, the means by which they function and how the data they consume is supplied is also discussed.

5.1 Prototype Overview

The DART prototype is the combination of a physical prototype and a digital control system, demonstrating its potential capabilities. Due to the operational requirements previously and later mentioned, collective as well as cyclic pitch control of the propeller blades is necessary, defining what kind of mechanism the physical prototype would entail, namely, a swashplate. A swashplate mechanism is one that provides both collective and cyclic pitch control and is widely used in helicopters. Below is an example of a swashplate mechanism:



Fig. 5.1A, Bo105 Rotorkopf, Bernd vdB, CC-BY-SA-2.5, Source

The way that the swashplate mechanism functions in DART's case is by translating the swashplate, the ring in the middle that connects the linkages, along one axis, namely vertically, and allowing it to tilt in any direction. The means by which the swashplate is actuated is through the use of TERRN.DYNAMIC'S ARC M1 closed-loop rotary actuators which were custom developed for the DART project. The actuation of the swashplate results in the two controls, collective and cyclic, being affected. Below is a breakdown of the movements and their effects:

• **Vertical Displacement of Swashplate:** Results in the collective pitch control. Assuming there is no tilt, this results in a uniform blade angle and the actuators are at the same angular position.

• **Tilting of Swashplate:** Results in the cyclic pitch control. Throughout a rotation, assuming that the swashplate is tilted, a propeller blade's angle is changed, allowing for the p-factor principle to be met. The actuators do not assume the same angle when the swashplate is tilted.

The prototype was designed and constructed vertically, strongly resembling what would be observed on a helicopter. However, it is crucial to note that this mechanism would be oriented horizontally on the main axle that drives the propeller. DART's swashplate mechanism was designed to allow for a 110° range of motion of the propeller blades, from 90° to -20° relative to the plane of rotation of the propeller, allowing for feathering and stationary full-reverse thrust mode. The specifics of these modes are discussed in the following sections.



Fig. 5.1B, Photo of the DART Prototype, Note Inaccurate Propeller Blade Orientation

Due to a design error, the placeholder propeller blades in the picture were oriented incorrectly. However, the simple physical interface through which the blades are connected allow for eased design iterations and revisions.

The goal of the prototype is to provide a tangible item to which all of the theory is attached, demonstrating how each parameter affects the conditions the propeller is under and how they are handled. The three actuators on the bottom are the ARC M1 actuators that are discussed in the following section. It was planned to utilize linear actuators, or put simply as pistons, instead of rotary actuators due to the decreased physical space it would ascertain. This would however prove difficult because of technical limitations regarding closed-loop control, forcing me to settle on the rotary actuator design.

5.2 Actuator Design

For driving the motion of the DART project and its swashplate mechanism, a motion control system was necessary. Hence, the Absolute Rotary Control, or ARC M1 closed-loop rotary actuator was conceptualized. There were multiple requirements that served as the outline for ARC's capabilities that are listed below:

- Precision: Due to the nature of which the ARC will be operating in, precise motion is key. Even though the ARC is not intended for end-use parts in aerospace, it still needs to uphold a minimum angular deviation.
- Integration & Compatibility: The ARC is required to be easily integrated into any system, both physically and logistically. The ARC will therefore be categorized by and fulfill the requirements of a Universal Integrated Actuator, or UIA. The purpose of a UIA is to provide seamless integration into any motion control system.
- Manufacturing Compatibility: Because of the capabilities located within the confines
 of a teenager's bedroom, the ARC's primary structural parts and custom-shaped parts
 will have to be created through additive manufacturing facilitated by a Bambu Lab A1
 fused-deposition modeling 3D-printer.
- **Reliability:** The manufacturing capabilities listed above give rise to issues relating to regular wear and tear of traditional plastic toothed-gears. A different approach is required to address this issue and is elaborated upon further in the paper.

The methods by which the ARC achieved the aforementioned requirements were carefully considered and executed. Firstly, the issue of precision was solved through the use of two components, a stepper motor and an absolute rotary encoder. A stepper motor does not operate in the same way as the usual DC or brushless motor. The stepper motor is designed to operate step-wise, meaning that rather than focusing on constant rotation, it rotates in discrete steps that result in precise angular displacements. A stepper motor often provides 200 full steps, resulting in a 1,8° rotation per step. However, these limitations are often overcome through the practice of microstepping where the coils inside of the motor are partially powered, resulting in so called half-steps, quarter steps, and other higher resolutions, resulting in more precise angular positioning. The precision of the stepper motor is then combined with an absolute rotary encoder that can sense the angle at which the main axle is situated. The AS5600 magnetic rotary encoder was selected for not only being able to read angular changes, but for also being able to read current angular positions, resulting in a high precision closed-loop system exempt from any regular calibration. Further details about the AS5600 are found in the next subsection, 5.2.1.

Moreover, the requirement of easy integration and compatibility was achieved in both a physical and digital sense using simple interfaces. The physical interface for mounting the ARC consisted of four holes arranged in a rectangular manner. This approach, while rudimentary, simplifies both the design and manufacturing process for any assembly that could utilize the ARC, including the DART prototype. To complement the easy installation, the digital interface, or the means by which a desired position is communicated to the ARC,

utilizes a PWM signal. This ensures widespread compatibility with a range of digital systems, addressing the requirement of easy integration, both physically and digitally.

In addition, despite the limited manufacturing capabilities at hand, the ARC circumvented logistical difficulties through the extensive use of additive manufacturing. This approach also enabled rapid iterative prototyping, allowing for minimal lead times between design or manufacturing errors.

Finally, reliability is a cornerstone in any component's final operational characteristics and determines its current and future use cases, especially in precision motion control systems. The use of a closed-loop system eliminating homing sequences accompanied by the relative ease of sourcing replacement parts due to most of them being manufactured in-house, results in ARC's reliable operation for the DART project's purpose. However, regarding the issue of wear and tear, a new gearing system was developed to increase the torque of the stepper motor while simultaneously not introducing traditional toothed-gear wear found in plastic gear systems in particular. This gearing system was referred to as SMD, the stacked magnetic drive. The SMD system utilizes magnetic fields located within close proximity to one another to mesh gears with each other. Instead of teeth, each gear features an array of equal-numbered magnets with alternating pole directions, greatly increasing slip-resistance. The gears are then displaced both vertically and horizontally from each other, letting the poles of the axially-magnetized neodymium magnets in each gear be in line with one another, assuming the greatest holding force. The arrangement of the magnets underwent several iterations with holding-torque tests in between each design modification. Over the course of four months, the average measured torque the SMD could withstand increased tenfold, from approximately **0,033 Nm** to **0,34 Nm**. This torque exceeded that of the stepper motor selected for the ARC. Below are illustrations of the SMD system implemented on the ARC and the arrangement of the magnets.

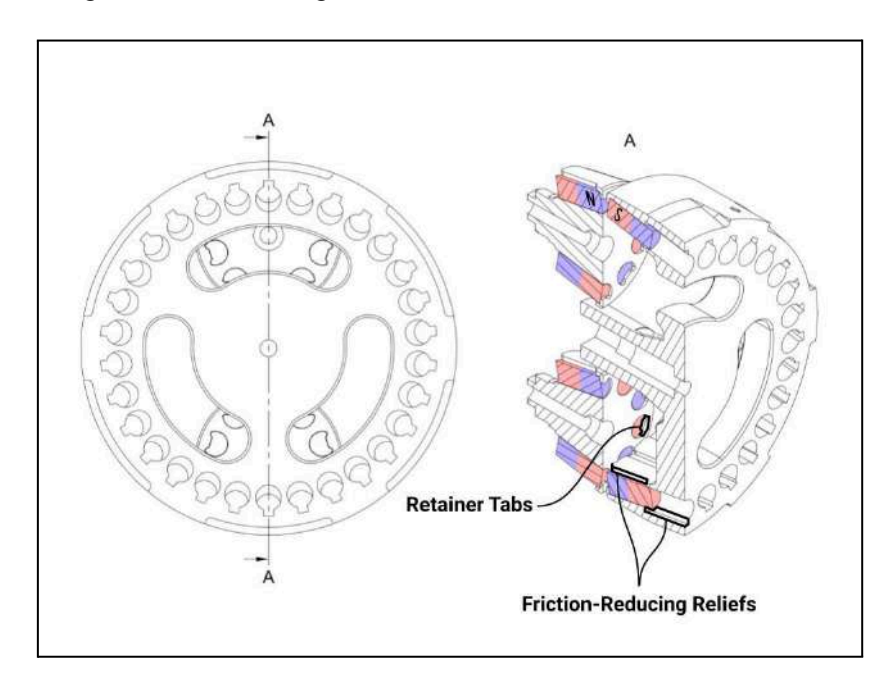


Fig. 5.2A, ARC M1 SMD Technical Drawing & Overview

In conclusion, the design of the ARC M1 closed-loop rotary actuator was defined by its operational requirements set by the DART project. However, there is a high likelihood of it being used in future projects due to its versatility and ease of use. Although it is relatively large for the amount of torque it can actuate, it is a step in the right direction and provides the crucial angular accuracy that the DART project relies on.

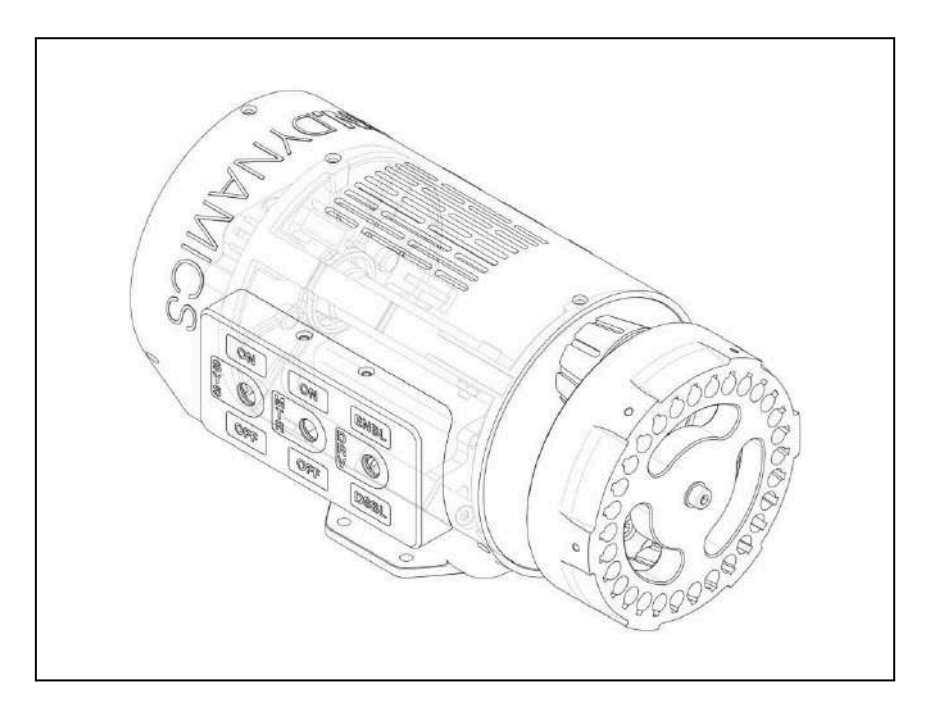


Fig. 5.2B, ARC M1 Technical Drawing Externals & Internals



Fig. 5.2C, ARC M1 Mounted on the DART Prototype

5.2.1 ARC M1 Systems & Electronics Overview

The ARC M1 comprises several smaller IC's that handle its operation, with the computations being performed on a Raspberry Pi Pico 2 located on the motherboard. The careful selection of the electronic components enables both closed-loop and precision control down to ±0,1° without needing any major initial calibration. The following list offers insight into the component selection and motivation.

- Raspberry Pi Pico 2: This microcontroller was chosen because of its widespread availability, wide array of various pinouts, previous personal experience using them, and its dual Cortex-M33 processors running at up to 150MHz. Raspberry Pi Ltd, 2024.
- **AS5600:** A breakout-board version was bought online to easily integrate it into the electronics. The AS5600 is a magnetic rotary encoder and was chosen because of its high-resolution 12-bit output and the ability to use the I²C communication protocol. ams, 2020.
- NEMA 11 Bipolar Stepper Motor: The stepper motor was manufactured and sold by STEPPERONLINE and it is the motor driving the actuator. This motor was chosen due to its naturally high precision due to it being a stepper motor, its low current requirements of approximately 0,7A, and its torque of approximately 12Ncm. STEPPERONLINE, n.d.
- TMC2208: A breakout-board version was bought online to easily integrate it into the
 electronics. The TMC2208 is a stepper motor driver that was chosen due to it placing
 heavy emphasis on noise reduction and smooth 1/256 interpolation, resulting in the
 fluid and quiet motion of the stepper motor being driven, alongside it being
 compatible with the specifications of the aforementioned stepper motor. Analog
 Devices, 2023.

The individual components are connected to each other through the use of a custom printed circuit board manufactured by JLCPCB. However, the AS5600 is connected to the circuit board via a cable due to it needing to be situated in close proximity to the actuator's primary axle's center of rotation. The use of a AS5600 magnetic encoder was seen as a potential risk due to the gearbox of the ARC M1 actuator being magnetically driven. However, further testing proved that it was not an issue and the actuator functioned within expected parameters. An air-cooling system was also implemented through designing air channels in the external cover of the ARC M1. This is to reduce to what extent the temperatures inside the actuator reach due to the stepper motor and the stepper motor driver in particular heating up over the course of their continuous operation.

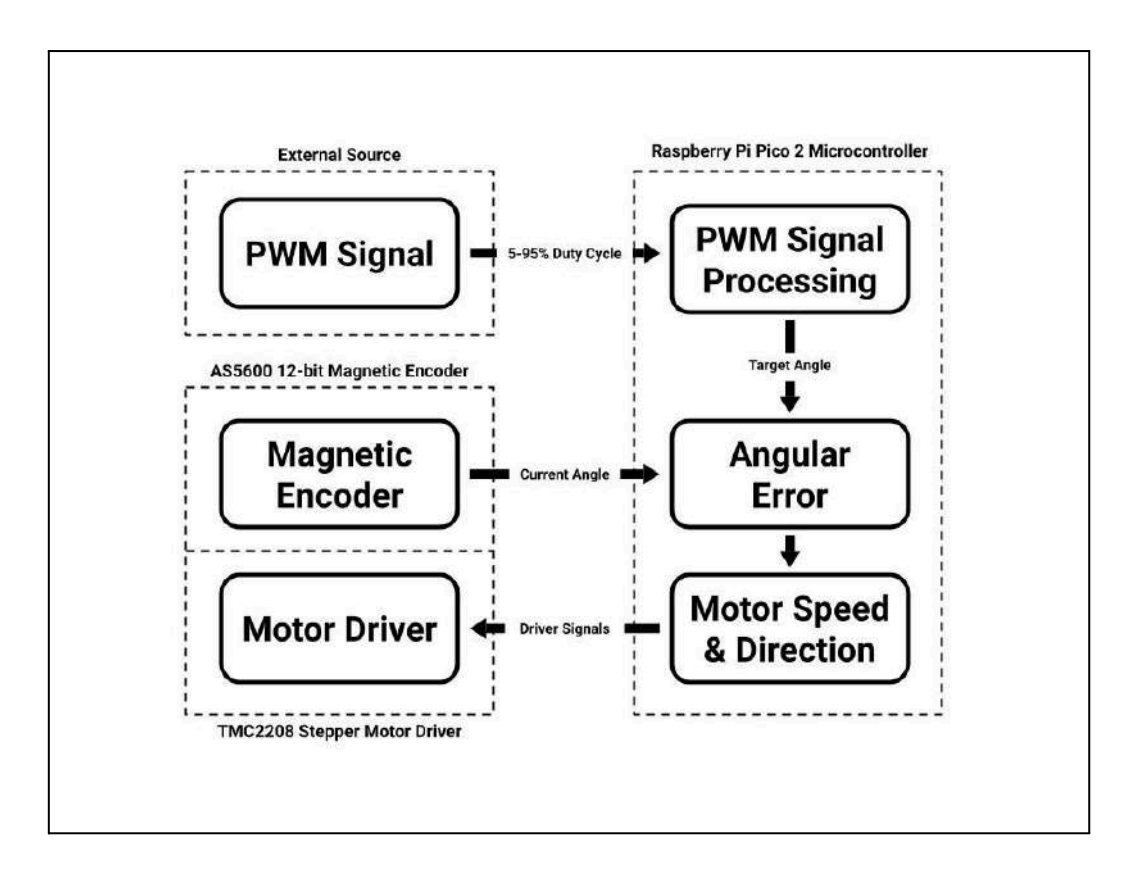
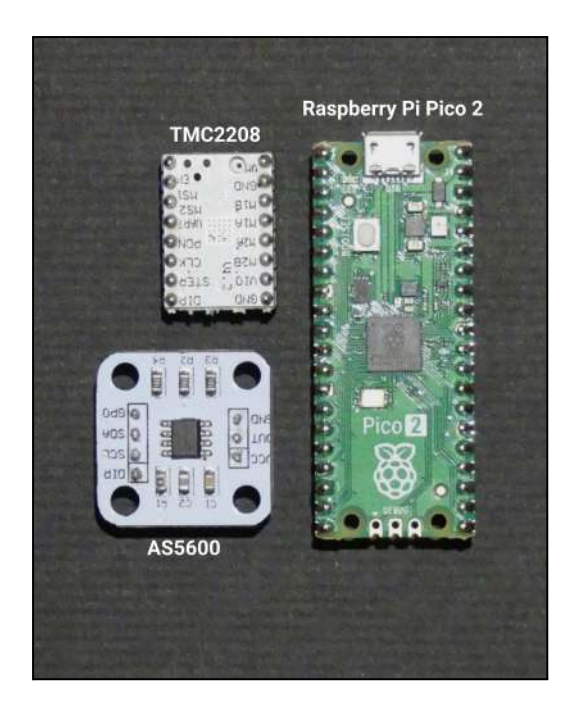


Fig. 5.2.1A, ARC M1 Systems & Components Overview

As shown in the graphic above, the individual IC's each serve a unique function in the ARC M1 actuator. The external source is any source that can provide a PWM, or pulse width modulated signal, that is processed and interpreted by the Raspberry Pi Pico 2 through the use of hardware interrupts. The interrupts are there to tell the microcontroller to immediately stop what it is doing to measure the length of the pulse provided by the external source. The length of the pulse is then converted into a value between 0 and 359,99 degrees to determine the target angle that the actuator is supposed to be at.

The AS5600 is then responsible for measuring at what angle the actuator is positioned in currently and sending it to the microcontroller. The difference between the target and current angle is then denoted as the angular error. The angular error determines in what the direction the motor is supposed to rotate and at what rate of angular speed it rotates. The microcontroller utilizes a separate PWM signal to generate the pulses that tell the driver to rotate the motor one step. The width of the pulses is only used to determine if the signal is actually sent or not, with a width of zero meaning that the signal is not sent and that the motor remains stationary. The use of hardware PWM signals is due to previously observed limitations of generating pulses through software.

The resulting control system is closed-loop and its hardware is primarily located on the motherboard. A power distribution board is also added to control where power is supplied and to enable control of back EMF and inductance from the stepper motor to prevent damaging the motherboard and its components under certain circumstances.





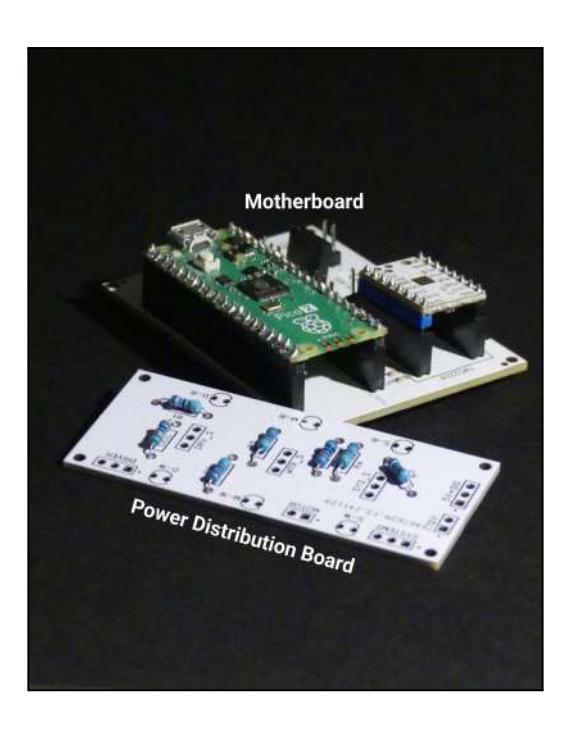


Fig. 5.2.1C, PDB & Motherboard

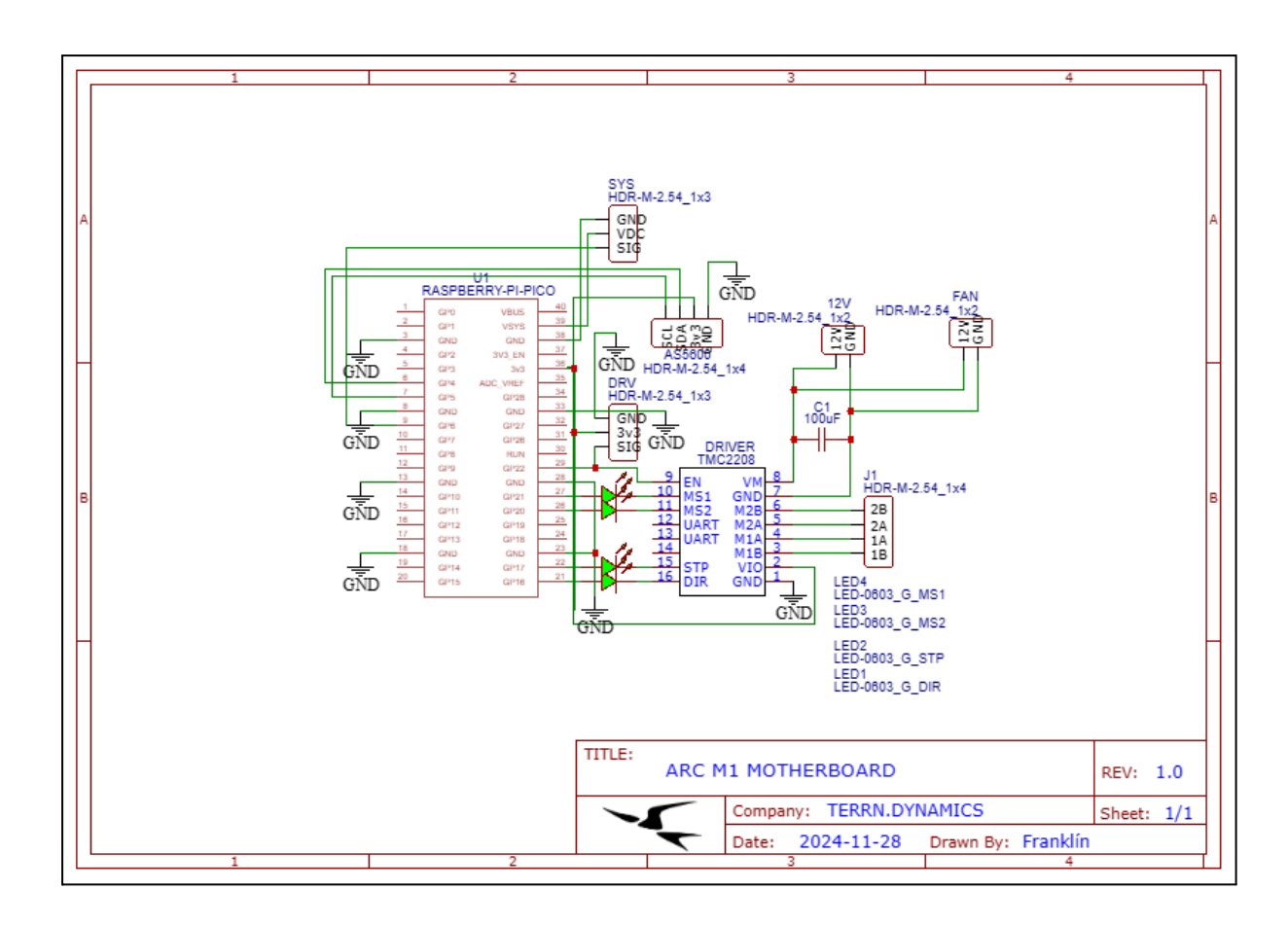


Fig. 5.2.1D, ARC M1 Motherboard Schematic

^{*}The schematic looks slightly like a mess but this was the result of four days of learning PCB design on my own, function over form are the wise words I went by.

5.3 Prototype Hardware Design

The design of the prototype hardware is very straight-forward compared to the multiple iterations that were done when designing the aforementioned ARC M1 actuator. As stated previously, the design is a modified swashplate mechanism, made to accommodate larger angular displacements of the propeller blades necessary to cover all functions of DART. The following list provides a breakdown of the primary components that form the DART prototype:

- **Base:** The structure that holds all the components together and supports the main axle that the propellers are attached to.
- Main Axle: Situated in the base and in the prototype simulates the physical connection between the propellers and the motor and is a load-bearing element.
- **Propeller Hub:** Located at the end of the main axle, it houses the bearings and the rotary plates that the propeller blades are attached to.
- **Swashplate:** Located between the base and the propeller hub with linkages attached to it. The top and bottom sides rotate independently, allowing for the stationary actuators to orient the swashplate while the propellers are rotating.
- **Cyclic Retainer:** A small piece that extends out of the axle and connects to the upper portion of the swashplate to keep it in phase.
- Rotary Actuator: Responsible for orienting the swashplate in order to achieve a
 desired propeller pitch. It is connected to the lower portion of the swashplate.

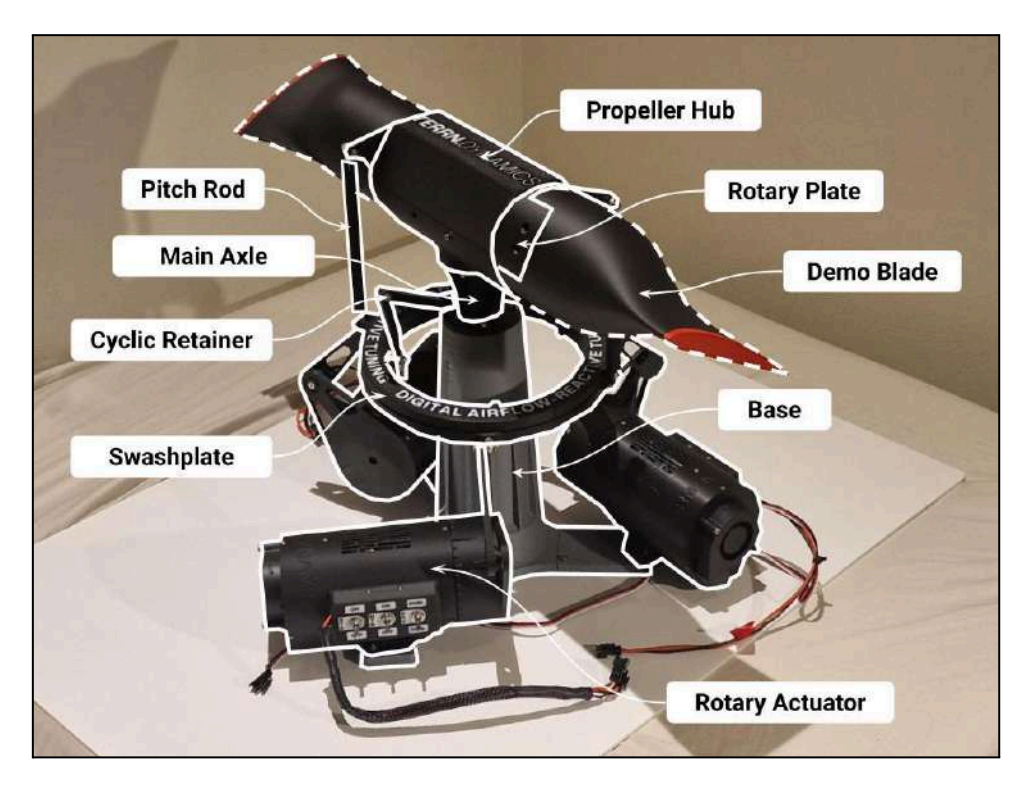


Fig. 5.3A, Overview of DART Prototype Components

5.4 Prototype Software Design

The software controlling the actuators and in turn, the propeller blades comprises three secondary systems, referred to as subsystems. These subsystems are arranged in a hierarchical order to clearly define their tasks and make any future adjustments easier to implement. The subsystems, in order of hierarchy, are:

- Phase-of-Flight (PoF): Responsible for monitoring the state of the aircraft and setting what performance characteristics the underlying subsystems adhere to. While considering an aircraft's airspeed, altitude, and orientation in three-dimensional space, control parameters are also taken into account to determine the current desired performance characteristics and the resulting propeller blade angle.
- P-factor Augmentation & Control Enhancement (PACE): Establishes specific cyclic
 pitch adjustments to either mitigate or generate p-factor turning moments based on
 the required performance characteristics set by PoF and the aircraft's orientation in
 the surrounding airflow. PACE modulates the propeller blade angle set by PoF to
 define to what extent the propeller blades should deviate from one another
 throughout their rotation.
- Digital Pitch Control System (DPCS): Collects the data provided by PoF and adjusts it
 based on PACE's instructions to determine the collective and cyclic blade angles.
 General sensor data from the aircraft are processed to establish the airflow vectors
 acting on the propeller blades and the resulting propeller pitch. With the established
 propeller pitch and inverse kinematics of the swashplate mechanism, DPCS sends
 signals to the actuators. The instructions from PoF and PACE are ignored if reverse
 thrust is selected or if an engine failure is indicated.

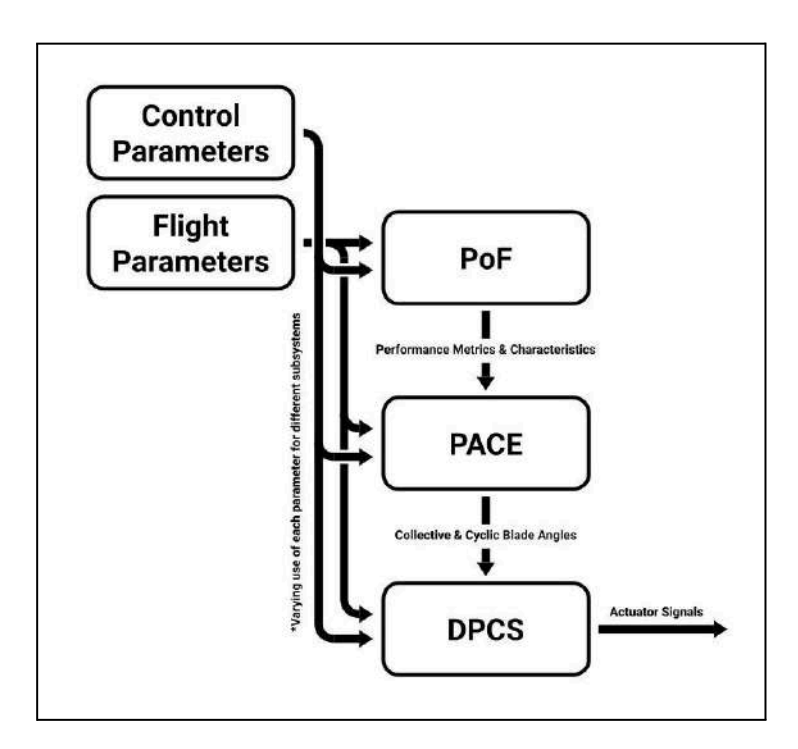


Fig. 5.4A, DART Subsystems Overview & Processes

5.4.1 Method for Modeling Optimal Alpha

The data that the numerical method by which the optimal angle-of-attack is estimated is derived from Xfoil digital airflow simulation results sourced from <u>airfoiltools.com</u>. The airfoil the prototype propeller will be utilizing is a Clark-Y asymmetric airfoil. There are two main metrics that are used to determine the airfoil's lift and drag, namely C_L v Alpha and C_D v Alpha. These metrics also have a corresponding Re attached to them, which is an additional parameter that the DART system relies heavily on.

The pieces of data collected from <u>airfoiltools.com</u> are scatter-plot where the individual alpha's are tested digitally, usually with a 0,25 degree interval between tests. A python program was written with the help of ChatGPT that can perform the regressions necessary to convert the discrete data points into mathematical functions that are utilized in future operations. A function was implemented in the program to be able to read the Comma Separated Value (.csv) formatted data files to eliminate the need for lengthy manual input. There had to be an initial decision for what regression will be appropriate for what metric, this decision was reached through visual assessment of original polar graphs. The resulting regressions that were needed to be performed were cubic for C_L v Alpha, and quadratic for C_D v Alpha. Below there are two graphs presented that illustrate the data points and the resulting regression attached to a specific Re, which in this case is 50.000. The graphs were created using matplotlib and the data was processed by the previously mentioned python program, Alpha is in degrees.

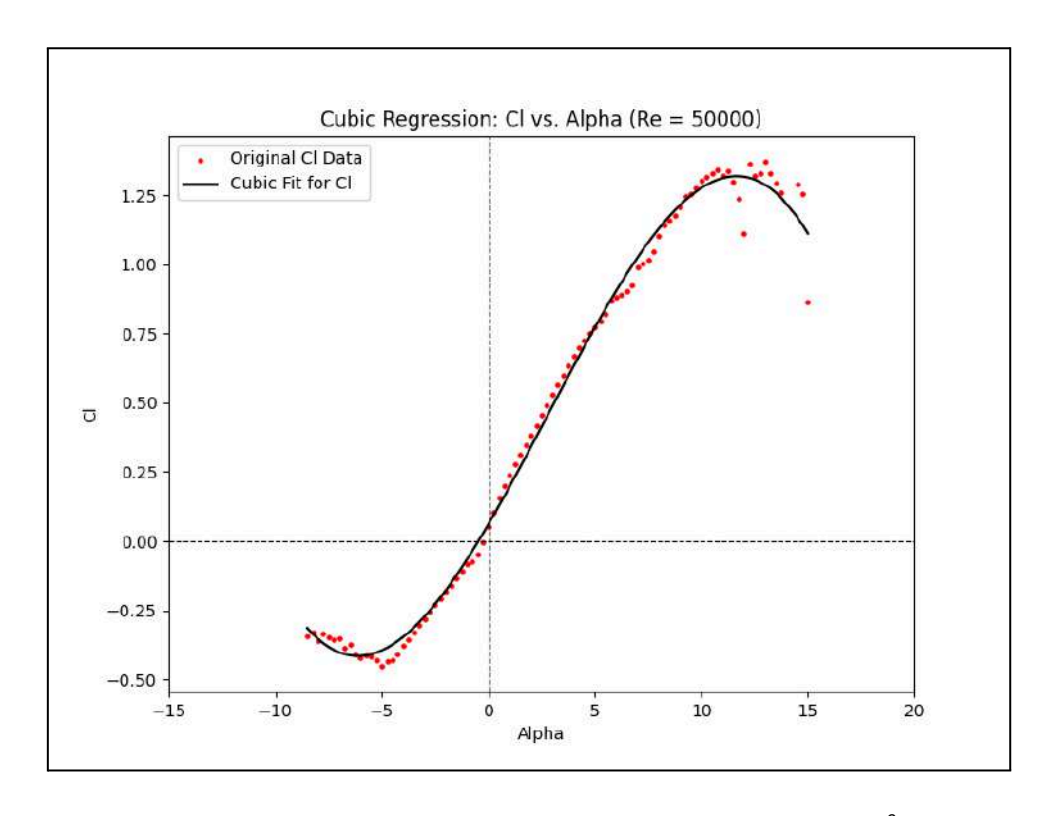


Fig. 5.4.1A, Cubic Regression of Clark-Y C_L v Alpha, Re = 50.000, $R^2 \approx 0.994$

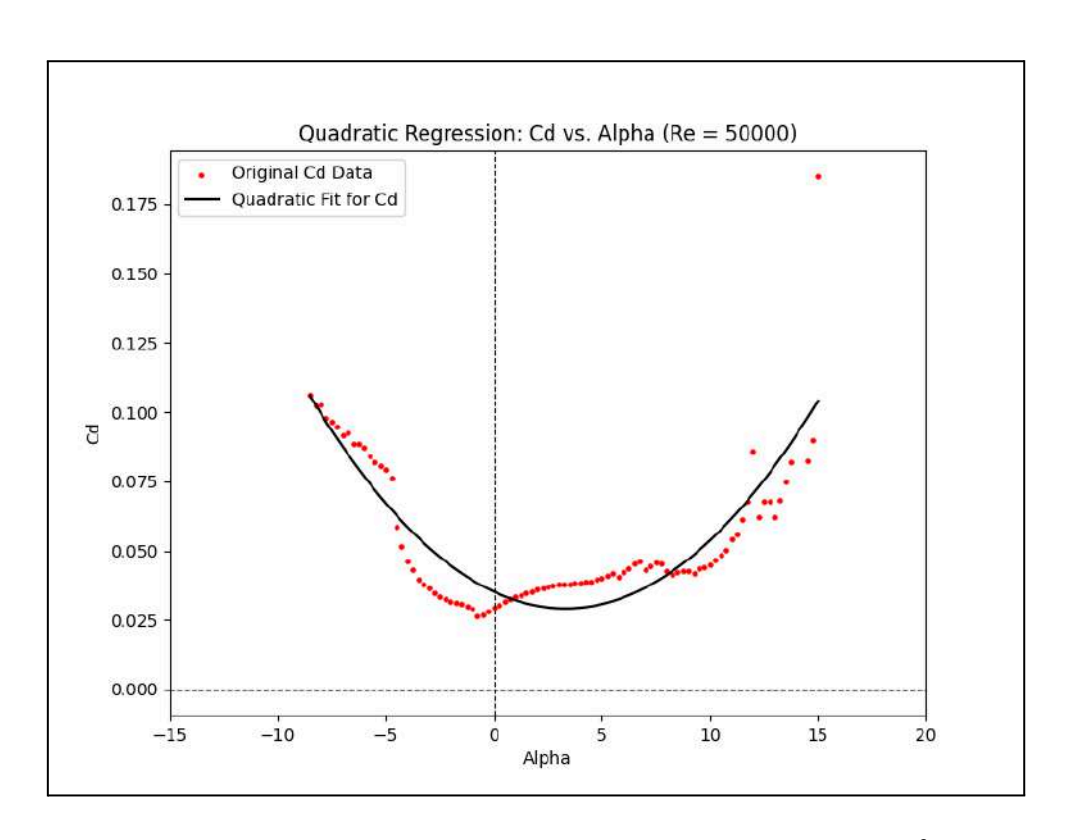


Fig. 5.4.1B, Quadratic Regression of Clark-Y $C_D v$ Alpha, Re = 50.000, $R^2 \approx 0.769$

The python program that performs the regressions is fed a .csv file that is provided by airfoiltools.com and takes note of what Re the data applies to. The data is also further processed by the program where the resulting function is compared to the original data points to establish the coefficient of determination, R^2 . This coefficient is used to describe how well a regression line reflects the actual data points, or put simply, how accurate the model actually is on a general scale of one to zero, where one indicates a perfect model and zero indicates a model that doesn't accurately reflect the data at all. ("Coefficient of Determination, R-squared", n.d.). While varying degrees in bias can be observed in both graphs, this is still within an acceptable range, considering the turbulent flow of a low Re. The optimal alpha is then determined by a C_L/C_D v Alpha function where the maximum lift-to-drag ratio is a peak with a specific alpha.

The process of extracting and interpreting data to produce two regressions, followed by an optimal alpha analysis through dividing the C_L v Alpha with C_D v Alpha as the y-axis with alpha as the x-axis to derive a maximum efficiency point, is repeated for the amount of airfoil data is available. In this case, the available Re airfoil data was 50.000, 100.000, 200.000, 500.000 and 1.000.000, resulting in five repeated calculations performed by the python program. The image on the next page illustrates the five C_L v Alpha functions at varying Re, representing how the lift is affected by how laminar the airflow is.

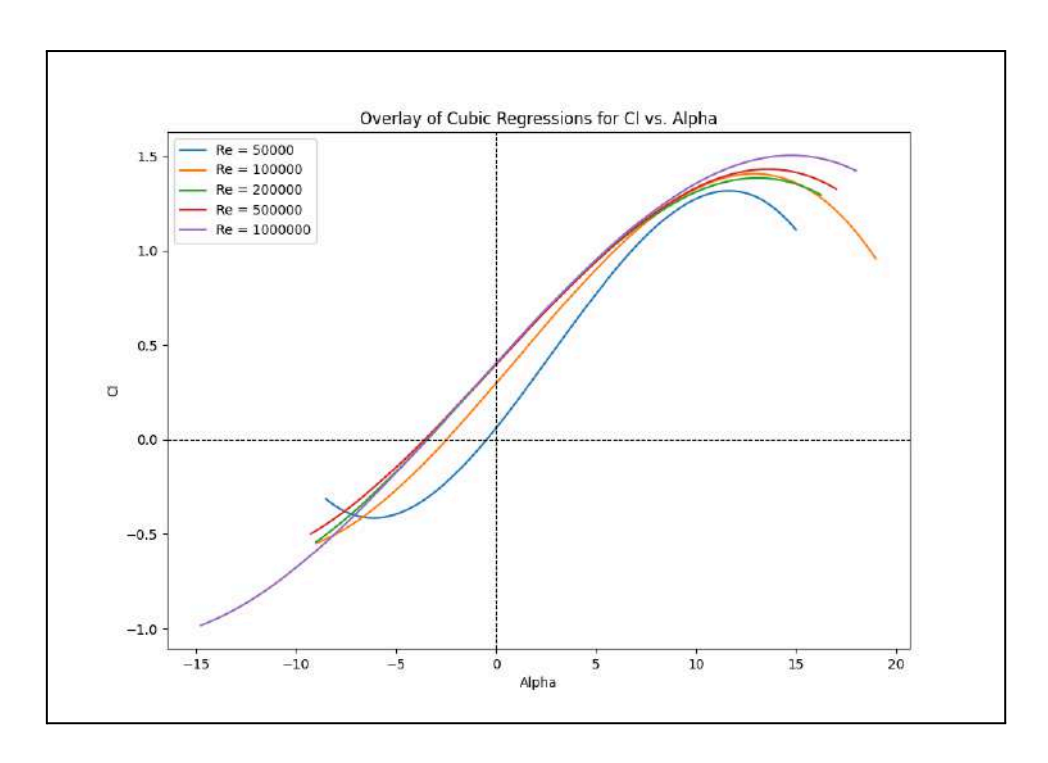


Fig. 5.4.1C, Clark-Y C_L v Alpha at varying Re

The optimal alpha is calculated in the python program and marked with a red dashed line as illustrated below. As was previously explained, the peak is where you get the most lift for an amount of drag. The drag in this case is a force that attempts to counteract the rotation of the propeller, leading to an increased load and a reduction in efficiency.

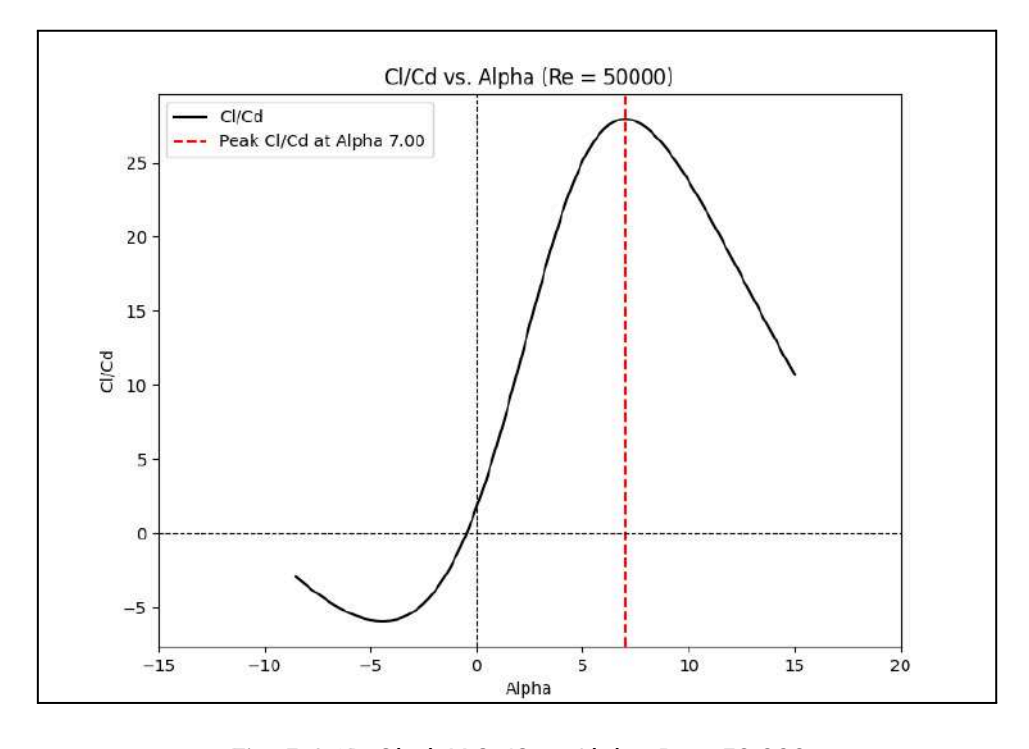


Fig. 5.4.1D, Clark-Y C_L/C_D v Alpha, Re = 50.000

The alpha at which the peaks are present are noted and plotted in an Alpha v Re graph where the optimal alpha is tied to the change in Re. The smooth transition between the efficient alpha's is crucial due to the Re experienced by the propeller varies drastically over the course of just one flight with parameters such as airspeed, pressure, and temperature fluctuating constantly. The exponential regression below representing Alpha v Re enables the system's smooth flight characteristics adjustments alongside an increase in the aerodynamic efficiency of the propeller blades.

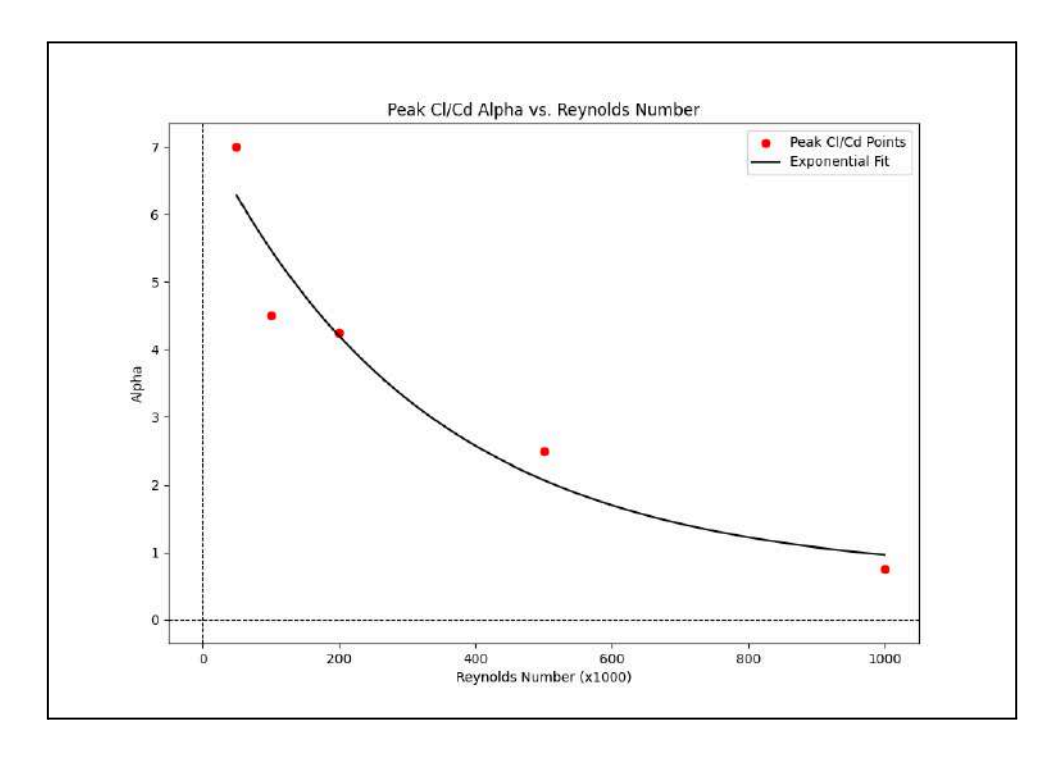


Fig. 5.4.1E, Exponential Regression of Clark Y Optimal Alpha v Re, $R^2 \approx 0.922$

The figure shown above represents the core of DART's potential efficiency gains where the optimal angle-of-attack is maintained throughout the numerous continuously shifting conditions the propeller blades are operating under. It is worth to note that all the graphs in this section alongside their respective data only applies to the Clark-Y asymmetrical airfoil, which is selected to be used in the prototype's reference propeller blade. Also, slight biases can be observed, with the C_D graph displaying it in particular. However, the deviations observed in low Re data and the lower Re end of Fig. 5.4.1E are results of the irregular nature of the turbulent airflow present at low Re values. It is important to note that the way and within what context the term "optimal alpha" is used is to describe the angle-of-attack that provides the most thrust for the least amount of drag. This is in stark contrast to the following sections where the sole focus is to achieve a high amount of thrust, disregarding the amount of drag it generates. While an optimal angle-of-attack is important during the climb, cruise, and descent phases of a flight, an angle that yields high thrust is crucial in critical phases such as the takeoff and landing where maximum performance is proven useful in adverse weather conditions or situations where high acceleration is necessary.

5.4.2 Method for Modeling High-Thrust Alpha

The method for how the high-thrust alpha is derived is very similar to the previous process. However, it seeks to determine the alpha that the C_L is at its highest for the same array of Re alongside a safety margin to account for adverse weather conditions in flight. There is an inherent risk of operating the propeller blade, or any wing profile, near its peak C_L where the airflow is highly turbulent and separates very early along the upper surface of the airfoil. Once the airflow is sufficiently turbulent and separated from the wing profile, the resulting loss of lift known as a stall follows. In the case of a propeller, the lifting force is the thrust.

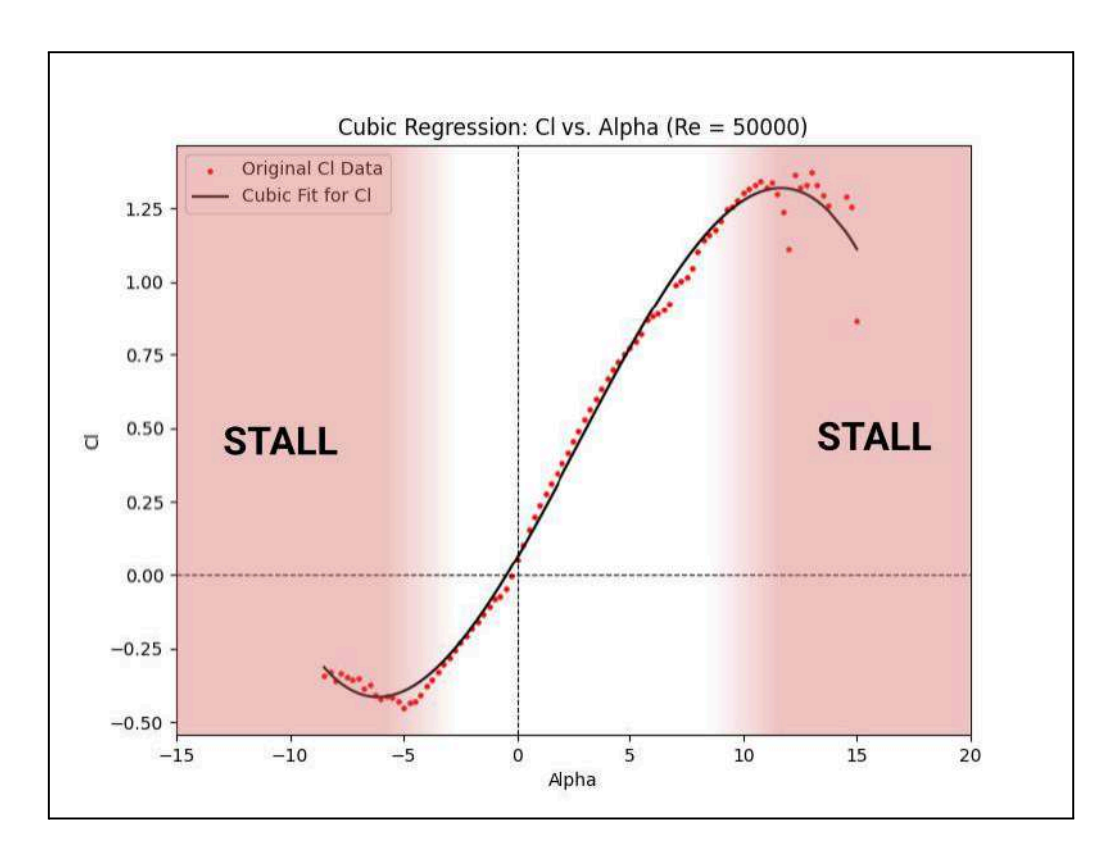


Fig. 5.4.2A, Clark-Y C_L v Alpha with stall zones illustrated

To reduce the risks of a stall occurring, two degrees are deducted from the peak C_L alpha value, allowing the angle-of-attack to briefly exceed its system-restricted maximum before the real-time system swiftly repositions the propeller blades. The use of a high-thrust alpha must be done sparingly. As mentioned previously, it is reserved for near-ground operations to maintain safety and efficiency. *Fig. 5.4.1D* illustrates the efficiency loss where the lift-to-drag ratio is roughly halved after passing an alpha of 12 degrees. The following page presents a C_L v Alpha graph that has the maximum and system-restricted C_L v Alpha values indicated.

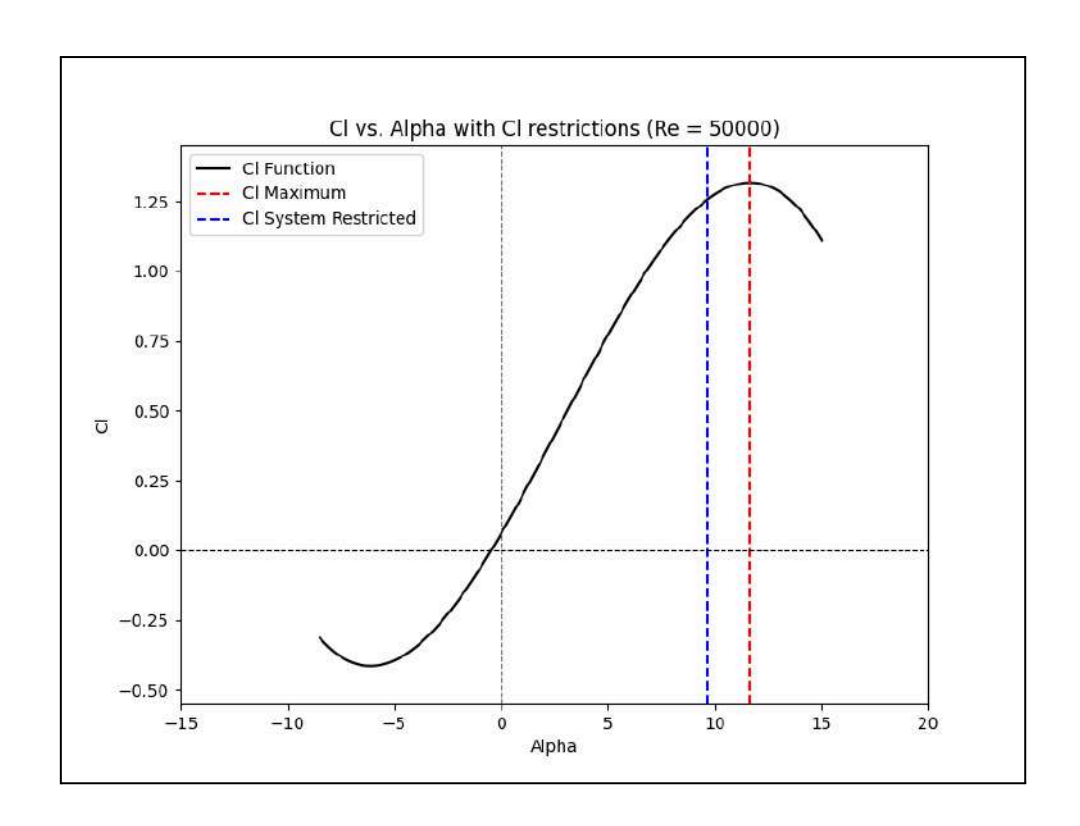


Fig. 5.4.2B, Clark-Y C_L v Alpha with C_L Maximum restrictions

With the system-restricted alpha values for the five sets of available Re data, the process of mapping the Re to a set alpha is repeated but utilizing the C_L system-restricted peaks instead of C_L/C_D peaks. The following high-thrust Alpha v Re graph is produced where a linear regression is performed, maintaining a high-thrust alpha regardless of a fluctuating Re.

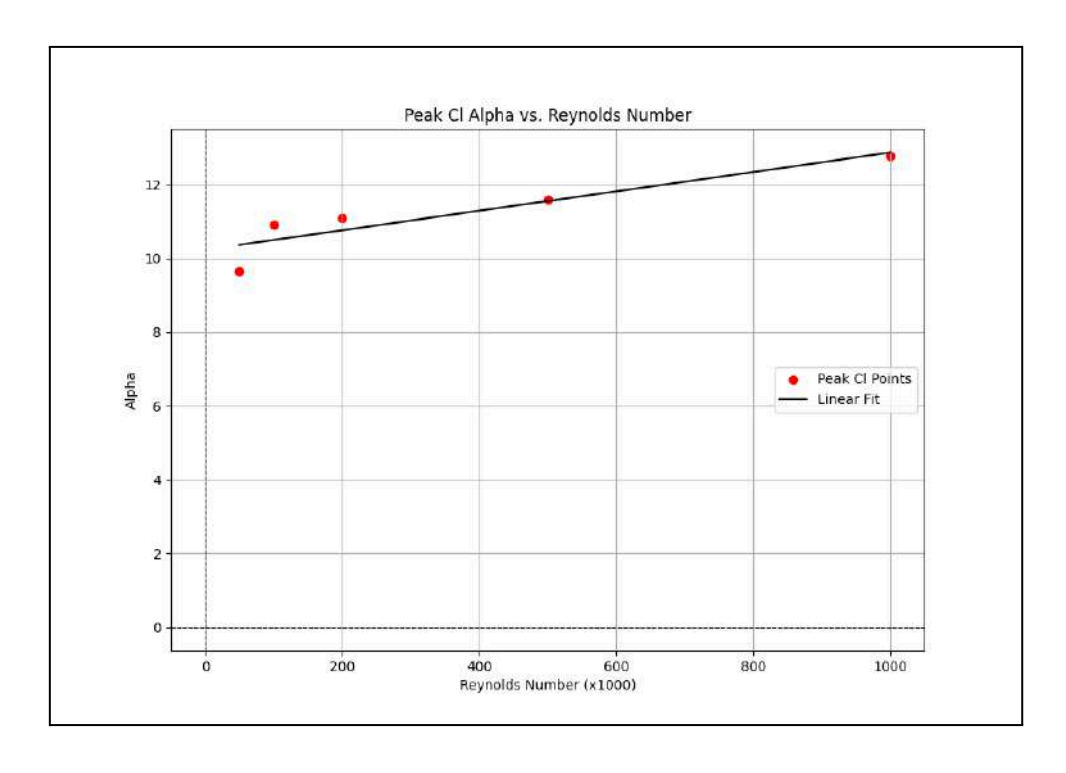


Fig. 5.4.2C, Linear Regression of Clark Y High-Thrust Alpha v Re, $R^2 \approx 0,786$

5.4.3 Method for Modeling Reverse-Thrust Alpha

Modeling the reverse-thrust alpha comprises an identical process for how the high-thrust alpha modeling was performed, except it seeks to identify the maximum reverse-thrust point, the minimum point in the C_L v Alpha cubic function. This is also followed up with a safety margin. However, the minimum system-restricted alpha will be one degree above the minimum because of the reduced risks associated within the context of reverse-thrust activation, entailing that an aircraft has detected weight-on-wheels and is in contact with the ground. It is important to note that the reverse-thrust alpha is not necessarily one with the highest drag. As explained previously, the drag on the propeller blade counteracts its rotation and not its forward thrust.

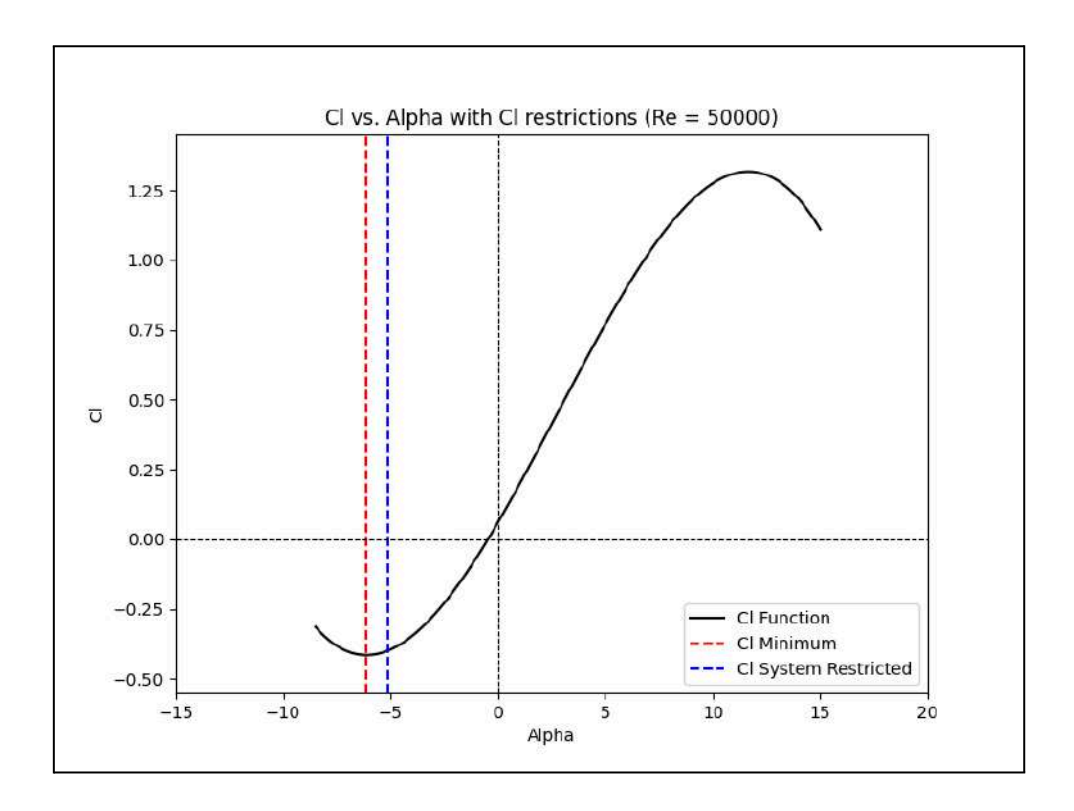


Fig. 5.4.3A, Clark-Y C_L v Alpha with C_L Minimum restrictions

The same regression as was done on the high-thrust Alpha v Re is performed in this model to allow for a continuous stable reverse thrust output from the propellers during landing and subsequent roll-out. It is crucial that the reverse thrust is effective to both increase safety as a result of shorter landing distances and operational efficiency due to the reduced wear the aircraft's brakes experience. On the next page is the final reverse thrust Alpha v Re graph, representing the most operationally efficient angles-of-attack at any given Re.

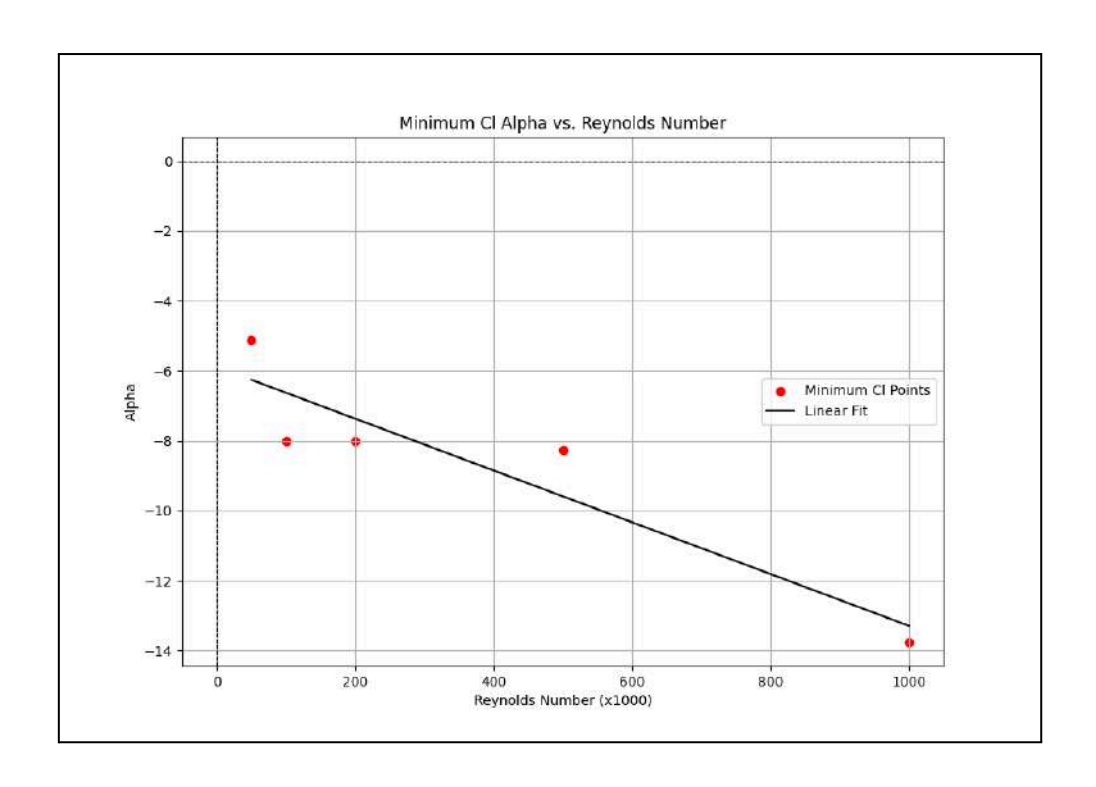


Fig. 5.4.3B, Linear Regression of Clark Y Reverse Thrust Alpha v Re, $R^2 \approx 0.854$

With the previous operation-oriented angle-of-attacks established, the overall and operationally efficient aspects of the DART project have now been outlined. The aim is to now implement systems that can accurately predict when each specific alpha is necessary and how it is achieved mechanically.

Note that there were limitations regarding the extraction of the minimum alpha due to the span of the data sourced from <u>airfoiltools.com</u>. This should not present too big of an issue though so it can be overlooked. Below is the original link to the Clark-Y airfoil data.

http://airfoiltools.com/airfoil/details?airfoil=clarky-il

5.4.4 Phase-of-Flight (PoF)

The Phase-of-Flight, or PoF, subsystem is responsible for overseeing the state of the aircraft and its control inputs to direct the DPCS to focus on maximizing efficiency or maximizing thrust. The way this information is conveyed is in the form of propeller modes, namely the efficiency mode and the power mode. PoF sits above all of the other systems and acts essentially like a conductor of the other systems. However, there are manual overrides to the PoF's commands that will later be discussed in the DPCS section.

The reason for needing to switch between modes instead of simply always maximizing efficiency is in the name of aircraft and passenger safety. In critical phases of flight, such as the takeoff or landing, it is paramount that we produce as much thrust as possible, both due to the mission at hand or potential dangers. When an aircraft commences a takeoff, the goal is to accelerate and increase our airspeed until a strong enough lifting force is generated by our wings. This is especially true when the takeoff is performed on a runway that is short where maximum thrust is often the only option. Therefore, due to the active requirement of a large acceleration, a mode for maximum thrust is necessary.

When an aircraft is in its approach and landing phase, maximum thrust generation is also highly desirable. This is due to two primary reasons. First, when landing, the aircraft is low and slow, this greatly increases the potential dangerous outcomes that issues such as an engine failure, bird strike, and gusty wind conditions can facilitate. If such an event would occur, it would be a necessity to have the maximum amount of power available at hand in order to safely mitigate the problem and avoid a potentially catastrophic accident. Second, at congested airports, or airports where there are adverse weather conditions present such as high and gusty winds, it is common that an aircraft has to perform a so-called go-around. This procedure can be performed for a number of different safety-related reasons, such as a failed landing attempt and not enough physical clearance between two aircraft. As the procedure's name suggests, it entails the aircraft going around and most often trying to land at the given airport again. However, it is common that a go-around also results in a climb and an increase in speed where the aircraft ascends to a safer altitude to avoid, for example, terrain. This poses yet again the requirement of high acceleration, positioning the landing and approach phases of flight to need maximum thrust if anything out of the ordinary were to happen. Below are the individual requirements, of which at least one has to be met, for the power mode to be activated, if none of these are met, efficiency mode is activated.

Landing Gear: Extended.

• Flaps: Extended.

Airspeed: Below a certain threshold, aircraft dependent.

• Thrust Setting: >95%.

In conclusion, the PoF system positions itself as sort of a safety mechanism acting in the interest of passengers and the aircraft, only enabling efficient flight when it does not pose a safety threat. Phases of flight where the efficiency mode is activated would be during the climb, cruise, and descent.

5.4.5 Digital Pitch Control System (DPCS)

The Digital Pitch Control System, or DPCS, is responsible for a large amount of the calculations, alongside generating the signals sent to the actuators driving the swashplate mechanism. The DPCS monitors the mode commanded by PoF while also monitoring parameters that override the PoF and PACE commands. Below are the two manual override situations and their respective reasonings behind the decision:

- Reverse Thrust: If reverse thrust is selected by the pilot, and the weight-on-wheels sensors indicate that the aircraft is in contact with the ground, PoF and PACE commands are ignored and the propeller blades are actuated to provide the maximum amount of reverse thrust. The angle at which the blades are actuated is determined by the alpha v Re function in Fig. 5.4.3B. This ensures that systems won't work against the pilots and that a landing and subsequent deceleration is achieved safely. This is an additional mode called the max-reverse mode, but it is not dictated by PoF.
- Motor Failure: If a motor failure is detected onboard and is communicated to DPCS, it ignores any and all DART system instructions and actuates the blades into so-called feathering. There are pre-determined angles for the actuators that actuate the propeller blades in such a manner as to have the least amount of drag possible, greatly reducing control issues and increasing the chances of a successful recovery and subsequent landing of the affected aircraft. A non-feathered propeller attached to a malfunctioning motor introduces huge amounts of drag to an aircraft in flight, and if the aircraft has two motors, a so-called twin-engine aircraft, the drag can result in large yawing moments, greatly decreasing controllability of the aircraft. For this reason, it was decided that DPCS will immediately prioritize the feathering of the propeller, in the name of passenger and aircraft safety.

For a given mode, DPCS selects the appropriate function detailed in sections 5.4.1 through 5.4.3 where the angle-of-attack of the propeller blade is such as to fulfill the current performance requirements. The main metric that determines what angle-of-attack is used is the Reynolds number, or Re, which is used in fluid dynamics to indicate how turbulent or laminar a flow is. The higher the Re, the less turbulent the flow is. The performance of the propeller blade and its associated airfoil depends heavily on this metric, where the higher the Re, the higher the angle-of-attack is generally needed to be in order to induce a stall as depicted in Fig. 5.4.2C, where a higher maximum C_L is possible through the increase of Re. However, the need to generate high thrust is only specified in the power mode, in contrast to efficiency mode, where an increase in Re results in an exponentially decaying optimum angle-of-attack, or alpha.

Reynolds number is heavily dependent on atmospheric conditions and parameters and throughout a flight, large variations in such conditions present themselves. Therefore, DPCS is delegated the task of dynamically calculating the Re based on common aircraft sensor data such as static pressure, IAS, and temperature. The means by which Re is calculated by DPCS involves an array of steps as detailed below in the order by which they are performed. The structure of the code was manually detailed with ChatGPT performing the programming.

- Computation of Air Density (ρ): The static pressure and temperature readings, alongside the specific gas constant for dry air, are fed into the ideal gas law formula that solves for air density (ρ).
- Computation of Dynamic Viscosity (μ): The temperature of the air, Sutherland's constant (S), and a reference viscosity (μ_0) at the temperature of 273,15 K (T_0) are fed into Sutherland's formula which yields the dynamic viscosity (μ) of the air at its current temperature.
- Computation of Kinematic Viscosity (v): The previously calculated dynamic viscosity (μ) and air density (ρ) are then used to compute the kinematic viscosity (v) of the air.
- Computation of Reynolds Number (Re): In this case, the relative velocity of the air times the average chord length of the propeller blade is divided by the kinematic viscosity which returns a resulting Re.

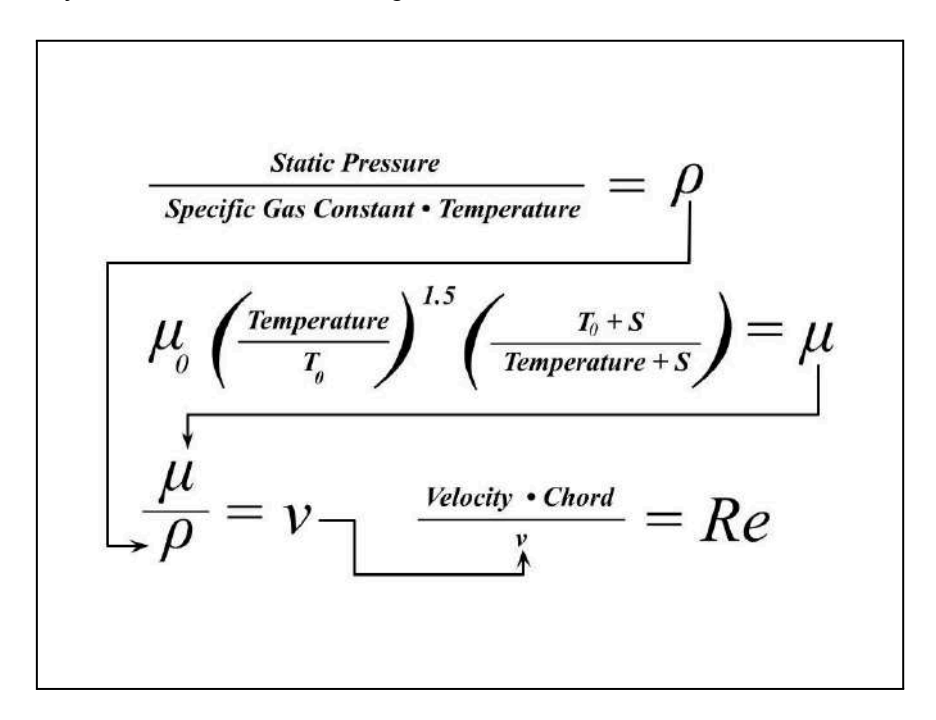


Fig. 5.4.5A, DPCS Reynolds Number Computation Process

The relative velocity of the air, used in the Re calculation, is determined purely through vector mathematics and the translation of IAS, indicated airspeed derived from dynamic pressure, into TAS, true airspeed, which compensates for atmospheric factors such as a high altitude or high temperature. The means by which TAS is calculated is not as multifaceted as the calculation of Re, below is the process that the DPCS program follows:

- Computation of Air Density (ρ): The static pressure and temperature readings, alongside the specific gas constant for dry air, are fed into the ideal gas law formula that solves for air density (ρ).
- Computation of True Airspeed (TAS): The true airspeed (TAS) is calculated through multiplying the indicated airspeed (IAS) by the root of the reference sea-level density of air (ρ_0) times the current air density calculated earlier (ρ) .

Static Pressure

Specific Gas Constant • Temperature

$$IAS \cdot \sqrt{rac{
ho_{_{0}}}{
ho}} = TAS$$

Fig. 5.4.5B DPCS True Airspeed Computation Process

In the DPCS system, the relative velocity mentioned in the final Re calculation step, is the hypotenuse of a right-angled triangle, where the horizontal side is TAS, and the vertical side is a function of the propeller's RPM at the radius of the mean chord of the propeller blade. These parameters are sourced from an aircraft's pre-existing on-board systems, further easing the implementation of the DART system into various pre-existing airframes.

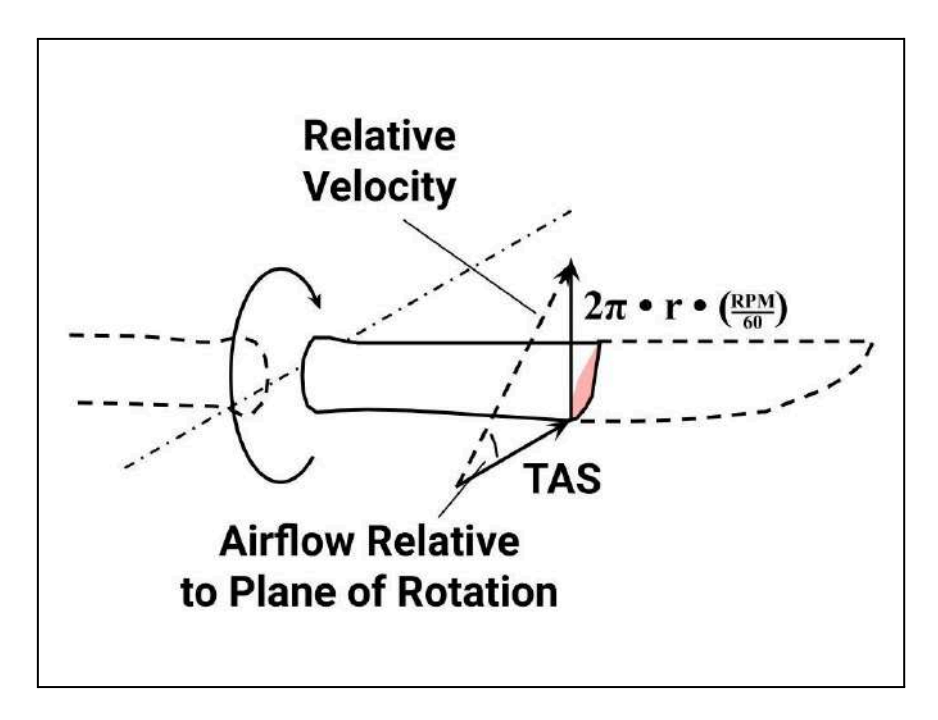


Fig. 5.4.5C DPCS Airflow Vector Computation Process

Alongside the scale of the hypotenuse, DPCS calculates the angle at which the airflow is hitting the plane of rotation, this is then compared to the current angle DPCS knows it has

actuated the propeller blade to relative to the plane of rotation, resulting in the known angle-of-attack of the blade. It was also planned to have the later mentioned subsystem, PACE, be able to augment the DPCS calculations before signals were sent to the actuators controlling the blade angles. The means by which PACE would be interacting with DPCS are discussed in the following subsection.

Finally, it was intended for DPCS to model the swashplate mechanism and calculate each of the actuator's angles for any given configuration through inverse kinematics and the modeling of a 3RRS (Revolute-Revolute-Spherical) parallel manipulator. However, due to technical and time-related constraints, it was decided that there would only be a collective blade angle adjustment which used basic trigonometry to map the actuator angles to any given height of the swashplate. Following the aforementioned computations, the blade angle relative to the plane of rotation is translated into the actuator's angular positions where it is communicated to the ARC M1's with the use of PWM. The process described in this subsection and its computations are performed over ten times a second, resulting in a real-time system that is responsive to the extremely dynamic nature of aviation.

5.4.6 P-factor Augmentation & Control Enhancement (PACE)

Although not realized in the prototype due to technical and time-related constraints, it is still beneficial to mention the concept and implementation of the P-Factor Augmentation and Control Enhancement system, also known as PACE. This subsystem would address control-related issues found on modern single-engine propeller-driven aircraft and UAV's by means which are not implemented today. The existence and the concept of the PACE system is the primary reason for the prototype's swashplate mechanism due to its ability to not only provide collective pitch control, but mainly cyclic pitch control.

PACE would add a layer to DPCS's complexity by reading the aircraft's angle-of-attack sensor, also known as the angle of attack vane. In the right-triangle vector calculation described in DPCS's Fig. 5.4.5C, it is assumed that the airflow stemming from the aircraft's linear movement forward is strictly horizontal. However, there are many cases where this airflow vector is not horizontal. PACE addresses this by reading the angle-of-attack and calculating the P-factor that results from the non-horizontal linear aircraft movement vector. P-factor is a direct result of the propeller blade's rotation, where in a simple two-blade propeller, one blade is always ascending when the other one is descending through their rotation. This poses an issue when the linear airflow stemming from the aircraft's forward movement is not horizontal, where one blade experiences an increased angle-of-attack while the other experiences a decrease in angle-of-attack, resulting in a difference in thrust generation. Due to their 180° phase shift, one side of the propeller disc generates more thrust than the other, producing asymmetric thrust, also known as p-factor. This asymmetric thrust results in a yawing moment and is often undesirable, often requiring manual control surface deflections.

PACE would counteract, and as discussed later on, even leverage this phenomena. If PACE were to counteract p-factor, it would utilize vector-based calculations similar to DPCS for both propeller blades and with the possibility of the linear airflow from forward aircraft movement being angled, to calculate the difference in angle-of-attack between the ascending and descending blade. This angular deviation would then be communicated to DPCS in the form of angular augmentation commands, describing how the blade's angles should change through their rotation which DPCS would translate into cyclic pitch. The same methods apply for how PACE would generate p-factor, however, the angular deviations would be controlled by the pilot's control inputs, generating asymmetric thrust that would aid in aircraft control.

The leveraging of p-factor through artificially generating it, has the potential to prove useful for smaller UAV's operating in adverse weather conditions such as high winds, alongside general maneuvering improvements stemming from the elimination of p-factor through PACE. The p-factor generation would not be not be active throughout an entire flight due to its aerodynamic inefficiencies. Rather, it was planned to have PACE continuously counteract the p-factor throughout a flight, while p-factor generation would be reserved for certain conditions such as PoF determining power mode necessary.

5.5 Technical Software Implementation

This section briefly discusses the technical implementation of the various subsystems and how they interact with each other on a superficial programming level. It is also mentioned how and from where the DART prototype sources its input data that the subsystems utilize.

5.5.1 Input Data Control

Due to regulatory hurdles associated with mounting components, especially control-related, on aircraft, the input data is simulated through an online form locally hosted on the Raspberry Pi 5 computer that the DART programs are stored and run on. On this site, flight parameters such as IAS, altitude, and angle of attack are able to be manipulated, alongside control parameters such as landing gear status, flaps, and thrust setting. The site, much like the programs, was structured by the author and programmed by ChatGPT. The upper portion of DART's Manual Data Intervention Interface, or MDII, is illustrated below:

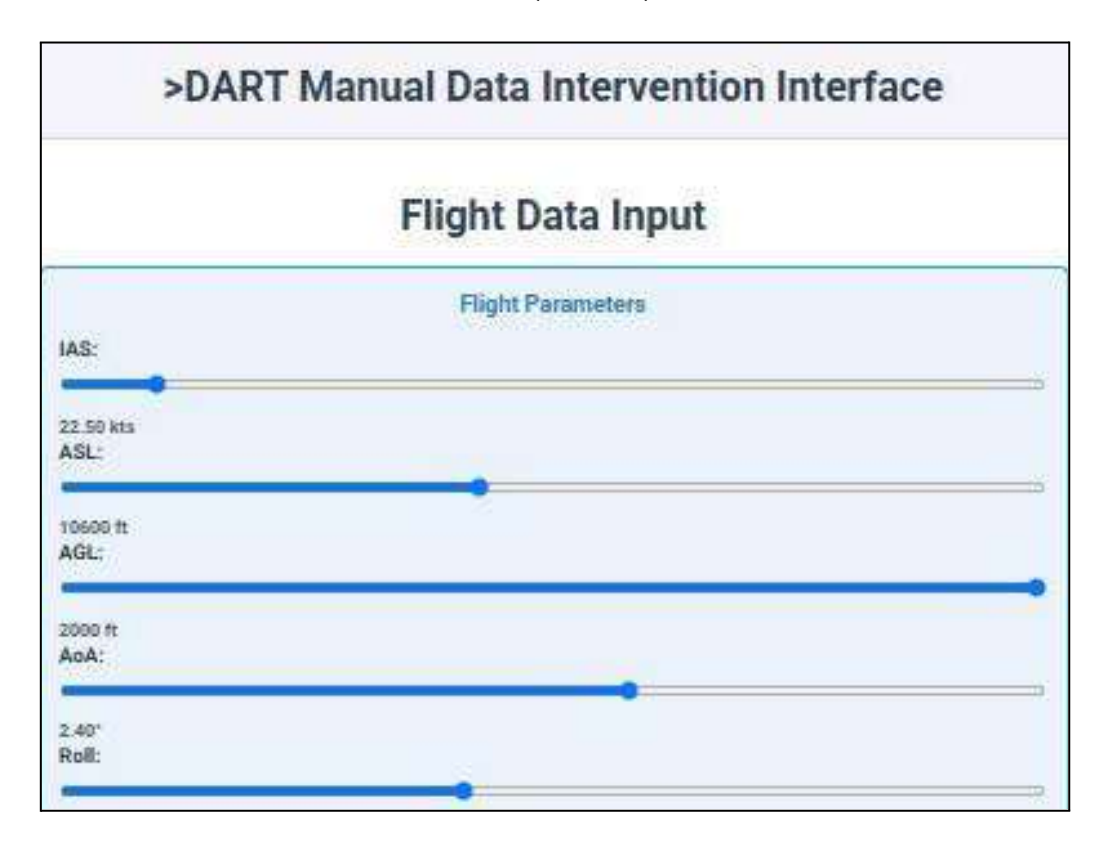


Fig. 5.5.1A Upper Portion of DART MDII

More technical parameters such as pressure and temperature are mostly connected to the ASL, or Altitude above Sea Level, slider in accordance with <u>ISA's standard atmosphere</u>. However, it is possible to also manually adjust these parameters after adjusting the ASL, adding another layer of prototype complexity and realism. A "MOTOR OK" parameter is also implemented in the MDII to provide DPCS with the cue to assume propeller feathering to demonstrate its swift response to safety-critical issues that are paramount to address in aviation.

5.5.2 Systems Integration

All of DART's systems, with the exception of the ARC M1 actuators, were written in Python. This programming language was chosen because of two reasons; firstly, I, as the author and the person behind this project, am familiar with Python and have a basic grasp of its syntax, enabling easier troubleshooting and catching errors. Second, it is popular due to its readability and general ease of use, with applications in automated systems, data-science, and prototyping (Kosourova, 2024), which is what DART is at its core.

The DART system runs on a Raspberry Pi 5 through three separate programs. The PACE system was skipped due to previously mentioned issues. Below is a list of the programs:

- **fetch_data.py:** This program is responsible for hosting the MDII while structuring and passing on the information in the form of two separate shared memory lists discussed later.
- pof_sys.py: As its name suggests, this is the PoF, or Phase-of-Flight system that reads and creates shared memory lists that provide information to the other programs.
- dpcs_sys.py: Again, as its name suggests, this is the DPCS, or Digital Pitch Control System. It reads all available shared memory lists and generates PWM signals that are sent out via a custom made Raspberry Pi 5 HAT, or Hardware Attached on Top, module.

These systems rely heavily on so-called shared memory functions, mainly in the form of lists. To retain the superficial nature of this subsection, shared-memory is a practice that lets multiple programs access information simultaneously, allowing for inter-program communication. In this case, python lists were created and attached to the shared memory for the subsystems to efficiently convey parameters to each other without affecting one another. Lists in python is a function where you can store multiple, separate pieces of data in one variable. This is highly efficient in DART's case where a lot of parameters need to be communicated. Each program is told what item in the list it should read and what the value or data means, enabling multiple programs to read and interpret the data present in that part of the list in the manner that best fits their needs. Below are the three lists that are located in shared memory and are actively used in DART:

- **flt_params:** Created and updated by fetch_data.py. This list stores the flight parameters that both pof_sys.py and dpcs_sys.py utilize to perform their duties. Data such as IAS, altitude, and if the motor is running are stored in this list as separate items.
- ctl_params: Created and updated by fetch_data.py. This list stores the control
 parameters that both pof_sys.py and dpcs_sys.py utilize to perform their duties. Data
 such as thrust setting, flaps, and landing gear status are stored in this list as separate
 items.
- **prf_params:** Created and updated by pof_sys.py. This list stores the propeller mode used by dpcs_sys.py, indicating if either efficiency or power mode is active.

These lists act essentially as billboards that the programs read and interpret at their own pace and time, preventing inter-system delays that could impact the crucial real-time performance of DART. Below are illustrations of the python lists and the planned technical python program layout. Note that PACE and its associated parameters are not currently technically implemented in the DART prototype at the date of writing.

```
flt_params = [
   11.56,
   3230.88,
    609.6,
    2.4,
    -11.1,
    68074.45,
    267.15,
   11112,
    false,
    false
1
ctl_params = [
    0,
    false,
   0,
    0,
   0,
    false
1
```

Fig. 5.5.2A Lower Portion of DART MDII Showing Python Lists

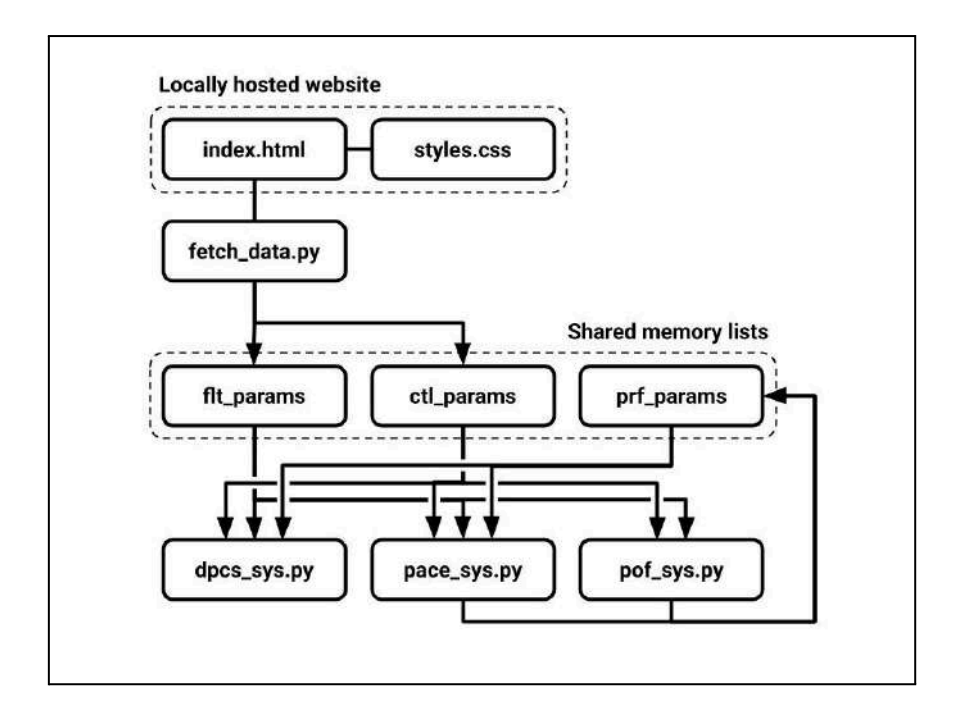


Fig. 5.5.2B Technical Python Program Layout of DART

The programs are started and run from the terminal in the Raspberry Pi 5.

6. Results

This section is a brief overview of what was achieved and an evaluation of the physical prototype performance, followed by a comparison between a fixed-pitch and DART-controlled propeller system. SimScale sponsored this project, providing the platform to facilitate digital wind tunnel testing.

6.1 Preliminary Prototype Performance

After assembling and programming the prototype, alongside some troubleshooting, observing the prototype moving as expected was a significant milestone. For example, the automatic feathering, or autofeathering, of the propeller, a critical safety feature, was responsive and acted right away as the "MOTOR OK" parameter was set to false on the MDII. When the user dragged a slider on the website, the prototype, without delay due to DART's real-time system structure, acted accordingly and set the blades to their suitable angular position.

However, the ARC M1 actuators exhibited some issues. Namely, after running for longer periods of time, they would start to rotate in the opposite direction of what they were supposed to, resulting in them getting stuck and oscillating about a certain angular position. The causes for this persistent issue are discussed in the following discussion section. Second, slight jittering could be observed at times, most likely due to errors reading the time-sensitive PWM signals.

In addition, due to the flexibility of the plastic material 3D-printed and used in the prototype, rattling and non-intended movement was observed from time to time, with the propeller spinning in particular yielding instabilities. As discussed before, the PACE system was not implemented due to technical and time constraints.

In conclusion, there were issues that need addressing, however, none of them were critical and DART's hardware and software proved that the real-time parameter-reactive control system was possible.

6.2 Digital Wind Tunnel Performance

The performance data described is a comparison between a DART-actuated propeller blade system to a fixed-pitch propeller. The fixed-pitch propeller is designed with a blade twist and angle that is most efficient at the true airspeed of 60 meters per second, 1600 RPM and with a propeller radius of 0,6 meters. The DART system uses the same propeller blade geometry as the fixed-pitch system, with the only difference being that DART can actuate around an axis to augment thrust characteristics. The blade angles tested in the DART system are largely based on calculations in line with the DPCS and PoF system. However, upon further aerodynamic analysis, blade angles outside the scope of previously thought limits were also tested and are detailed in section 6.2.2. It is important to note that lift and drag in this context are the forward thrust and resistive aerodynamic torque forces of the propeller.

The operating conditions chosen to have the propeller systems tested under are supposed to be representative of a high-performance UAV flight envelope. The conditions are the following:

- 5 m/s TAS & 2000 RPM: Early takeoff roll.
- 30 m/s TAS & 2000 RPM Rotation speed & early climb, potentially also a go-around scenario.
- 45 m/s TAS & 1800 RPM: Climb, descent, and approach.

Since this comparison is between a cruise-optimized propeller blade and DART, there would be no differences to actually measure. However, any change in cruise conditions such as an increased airspeed or RPM would lead to inefficiencies that could be addressed by DART.

Finally, the airflow, along with its turbulent kinetic energy (TKE), is analyzed and presented as well as the pressure distribution over the blade itself in the form of a superficial observation. A more in-depth analysis is performed in the discussion section of this paper.

Prop Type	TAS (m/s)	RPM	Scenario	Thrust (N)	Drag (N)	Thrust/Drag Ratio	DART Ratio Increase	Thrust	Drag
Fixed-Pitch	5	2000	Early Takeoff	143,8	137,8	1,044			
DART (12,77 α)	5	2000	Early Takeoff	60,1	21,8	2,757	164,19%	-58,21%	-84,18%
Fixed-Pitch	30	2000	Rotation	164,5	150	1,097			
DART (12,77 α)	30	2000	Rotation	126,6	82,9	1,527	39,25%	-23,04%	-44,73%
Fixed-Pitch	45	1800	Climb	133	125,5	1,060			
DART (0,75 α)	45	1800	Climb	52,2	43,8	1,192	12,46%	-60,75%	-65,10%
DART T/O alphas	TAS (m/s)	RPM	Scenario	Thrust (N)	Drag (N)	Thrust/Drag Ratio	DART Ratio Increase	Thrust	Drag
Fixed-Pitch (Baseline)	5	2000	Early Takeoff	143,8	137,8	1,044			
DART (25 α)	5	2000	Early Takeoff	116,8	55,2	2,116	102,77%	-18,78%	-59,94%
DART (30 α)	5	2000	Early Takeoff	130,2	72,9	1,786	71,15%	-9,46%	-47,10%
DART (35 α)	5	2000	Early Takeoff	133,9	94,4	1,418	35,92%	-6,88%	-31,49%
DART CLB alphas	TAS (m/s)	RPM	Scenario	Thrust (N)	Drag (N)	Thrust/Drag Ratio	DART Ratio Increase	Thrust	Drag
Fixed-Pitch (Baseline)	45	1800	Climb	133	125,5	1,060			
DART (5 a)	45	1800	Climb	85,9	73,7	1,166	9,98%	-35,41%	-41,27%
DART (10 α)	45	1800	Climb	119,2	108,5	1,099	3,67%	-10,38%	-13,55%

Fig. 6.2A General Performance Comparison Overview

6.2.1 Mathematically Governed Thrust Performance Data

The performance data seen here are the direct results of the DPCS and PoF systems, using the given airfoil polar data and mathematical regressions to decide on the best angle-of-attack and actuate upon them. Note that drag is in N and not Nm, this doesn't have an effect on the comparison since the fixed-pitch and DART thrust characteristics are measured identically. These numbers are derived from Simscale's incompressible flow simulations.

Prop Type	TAS (m/s)	RPM	Scenario	Thrust (N)	Drag (N)	Thrust/Drag Ratio	DART Ratio Increase	Thrust	Drag
Fixed-Pitch	5	2000	Early Takeoff	143,8	137,8	1,044			
DART (12,77 α)	5	2000	Early Takeoff	60,1	21,8	2,757	164,19%	-58,21%	-84,18%
Fixed-Pitch	30	2000	Rotation	164,5	150	1,097			
DART (12,77 α)	30	2000	Rotation	126,6	82,9	1,527	39,25%	-23,04%	-44,73%
Fixed-Pitch	45	1800	Climb	133	125,5	1,060			
DART (0,75 α)	45	1800	Climb	52,2	43,8	1,192	12,46%	-60,75%	-65,10%

Fig. 6.2.1A Mathematically-Governed DART Performance v Fixed-Pitch Table

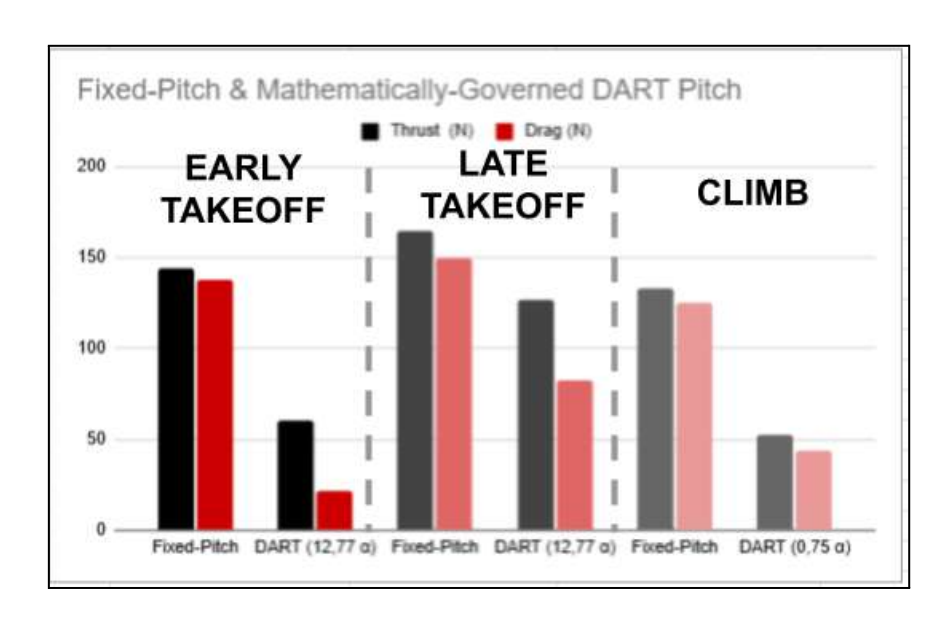


Fig. 6.2.1B Mathematically-Governed DART Performance v Fixed-Pitch Graph

6.2.2 Revised Thrust Performance Data

The performance data below in Fig. 6.2.2A are reactions to the aerodynamic performance of the mathematically governed blade angles. This data is more within an acceptable margin of performance metric changes. It takes into consideration the operational requirements of the aircraft itself rather than just focusing on minimizing torque forces resisting the propeller's rotation.

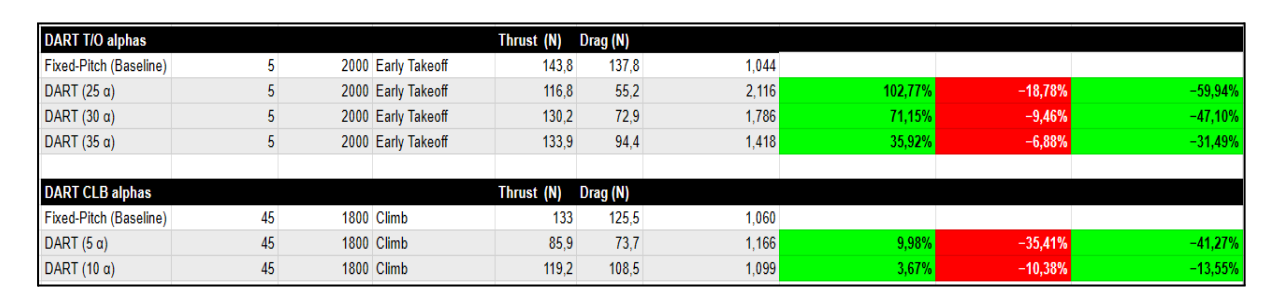


Fig. 6.2.2A Revised DART Performance v Fixed-Pitch Table

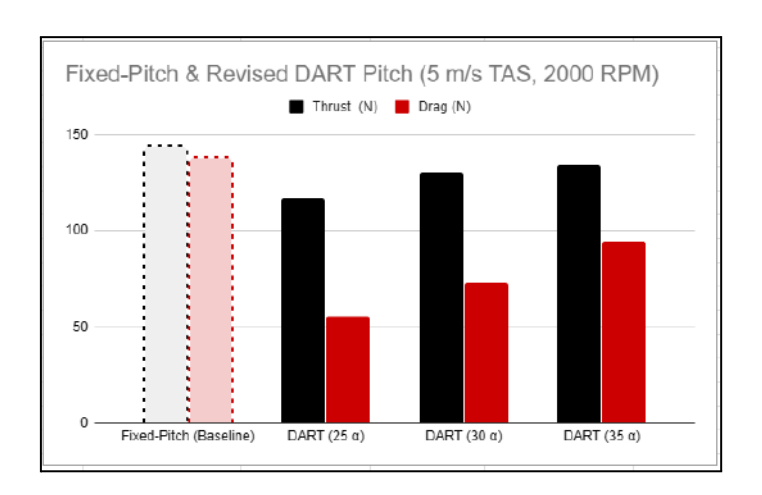


Fig. 6.2.2B Revised Takeoff-Oriented DART Pitch v Fixed-Pitch

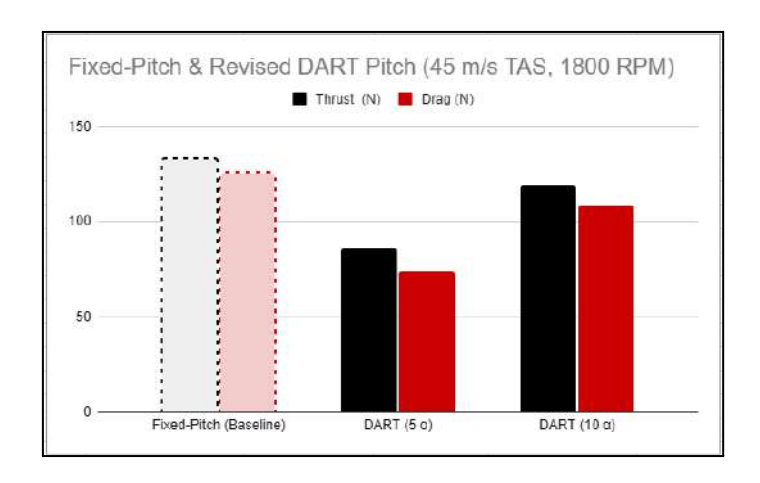


Fig. 6.2.2C Revised Climb-Oriented DART Pitch v Fixed-Pitch

6.2.3 Turbulent Kinetic Energy Represented Airflow

Presented are CFD simulation results of the fixed-pitch where the coloring is representative of the turbulent kinetic energy (TKE) present in the given airflow streams. The CFD simulation platform was provided by our sponsor, SimScale. The comparison is between the fixed-pitch propeller and the DART system with a target of 25 α in an early takeoff scenario.

*Fixed-pitch propeller presented below.

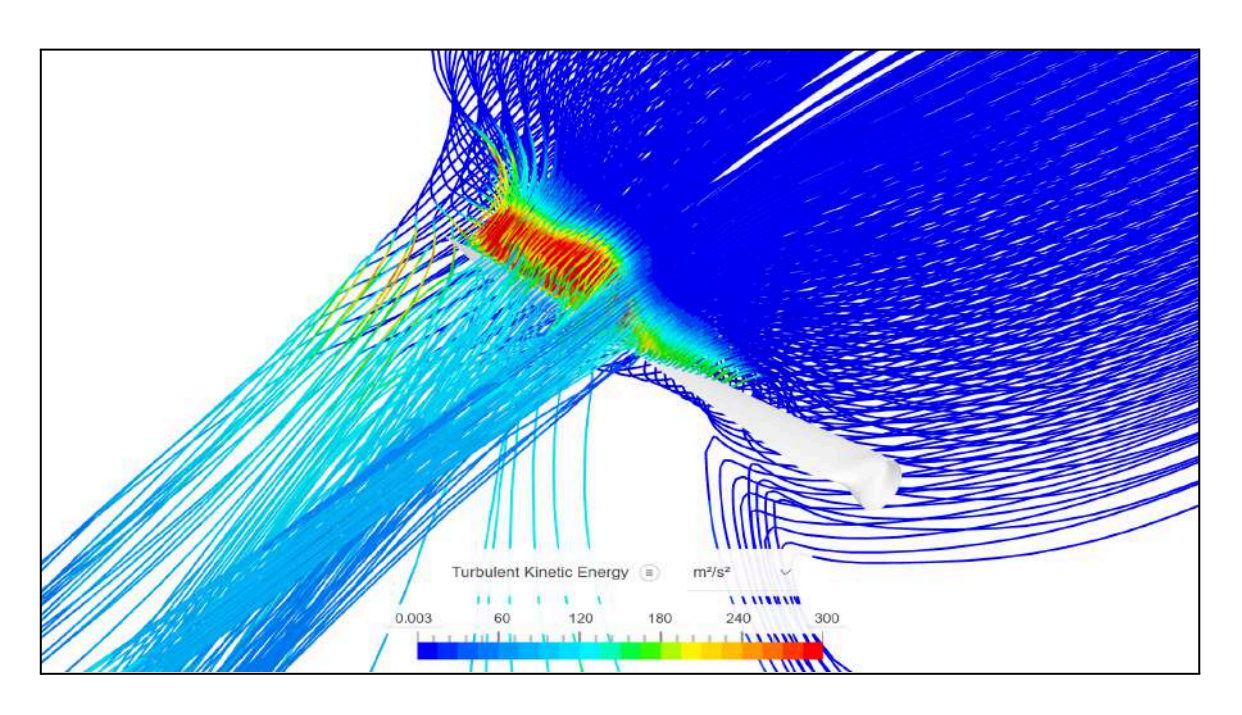


Fig. 6.2.3A TKE-Colored Airflow Analysis of the Cruise-Optimized Fixed-Pitch Propeller.

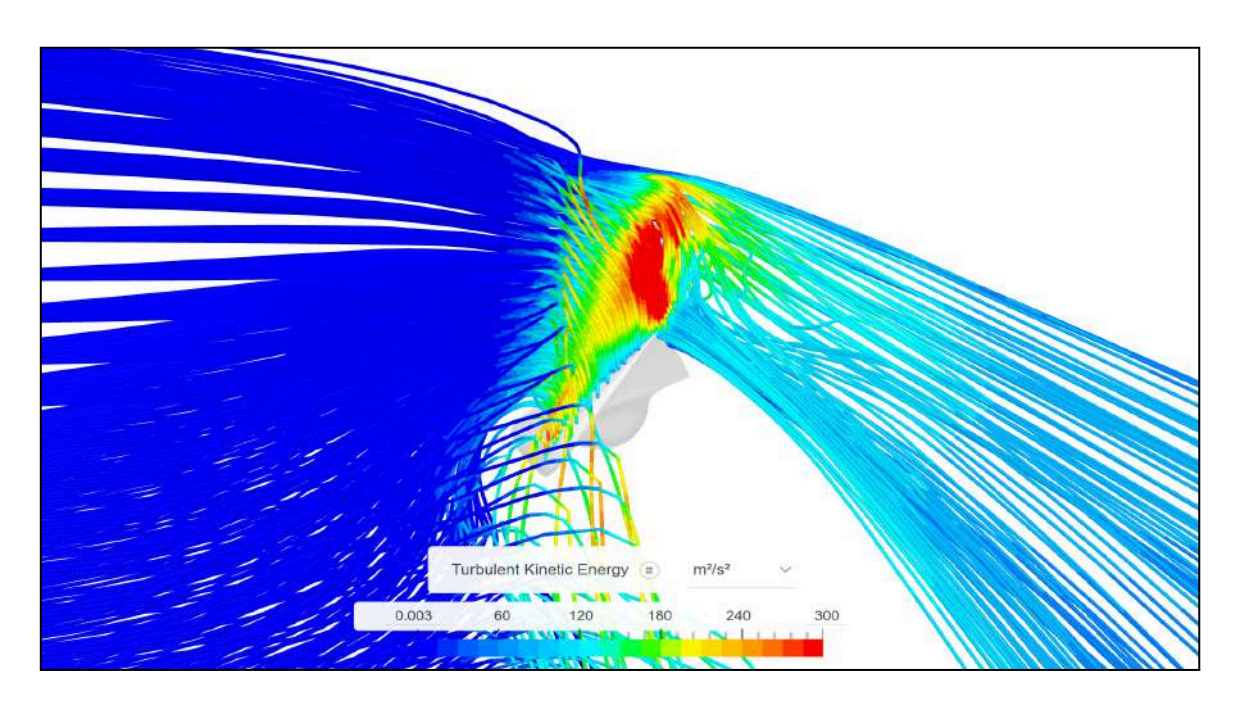


Fig. 6.2.3B TKE-Colored Airflow Analysis of the Cruise-Optimized Fixed-Pitch Propeller.

*DART regulated propeller presented below.

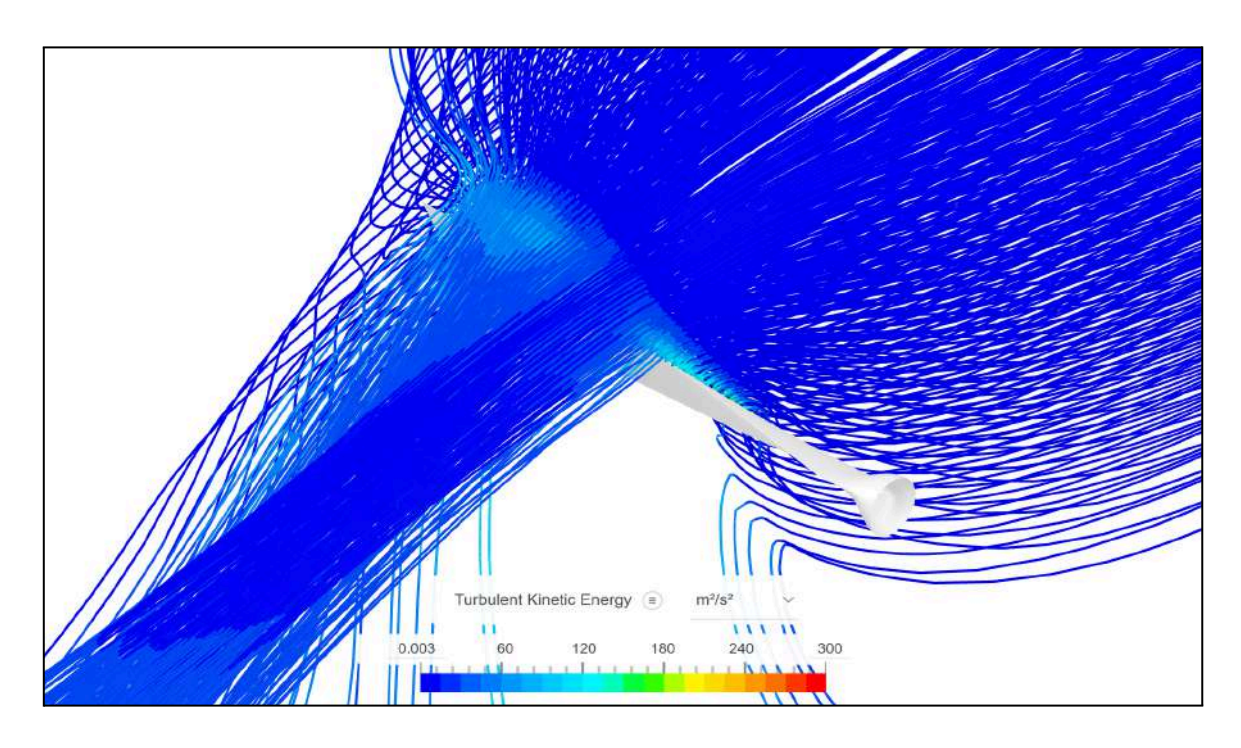


Fig. 6.2.3C TKE-Colored Airflow Analysis of the ${\it DART}$ Controlled 25 α Propeller.

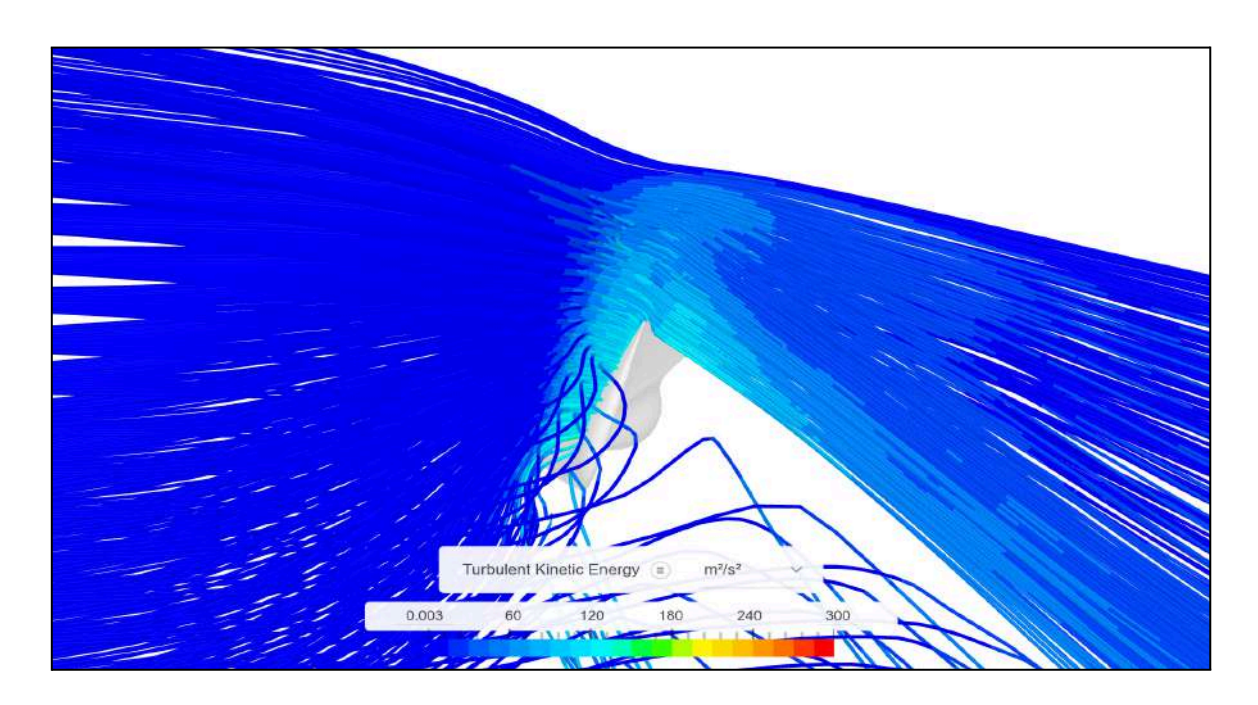


Fig. 6.2.3D TKE-Colored Airflow Analysis of the **DART** Controlled 25 α Propeller.

6.2.4 Velocity Represented Airflow

Presented are CFD simulation results where the coloring is representative of the velocity present in the given airflow streams. The CFD simulation platform was provided by our sponsor, SimScale. The comparison is between the fixed-pitch propeller and the DART system with a target of $25\,\alpha$ in an early takeoff scenario.

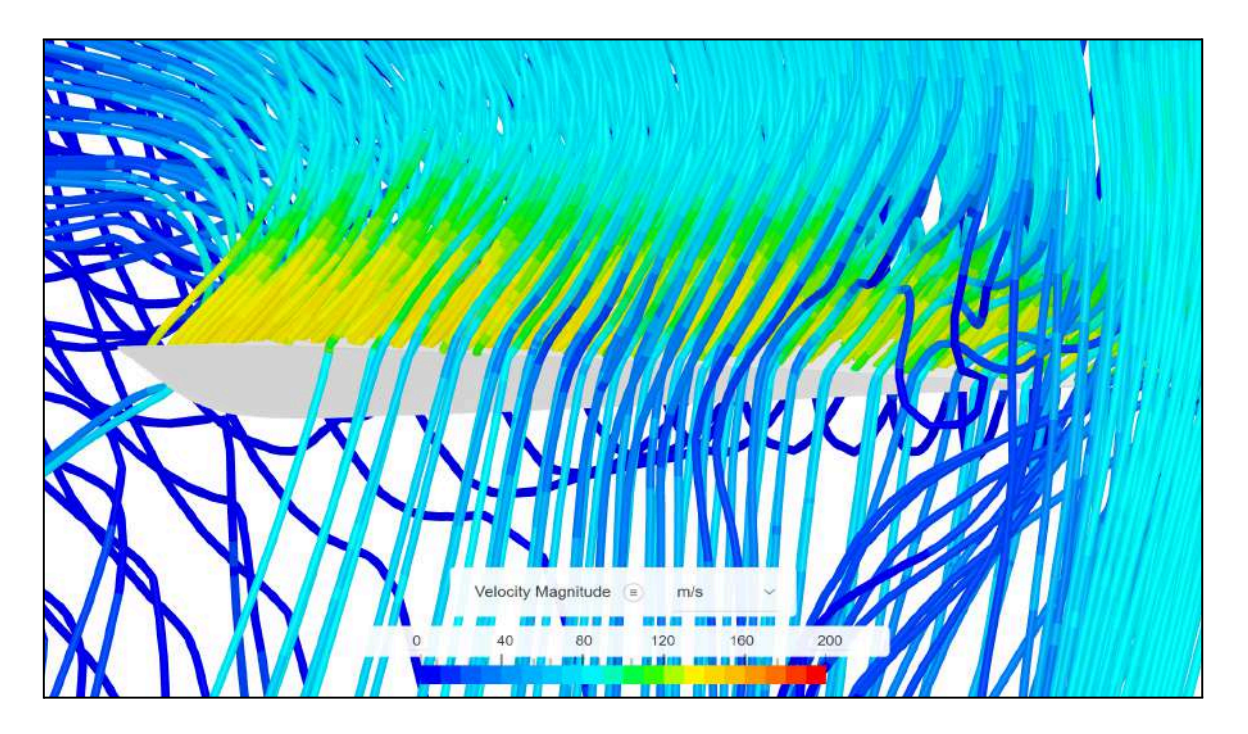


Fig. 6.2.4A Velocity-Colored Airflow Analysis of the Cruise-Optimized Fixed-Pitch Propeller.

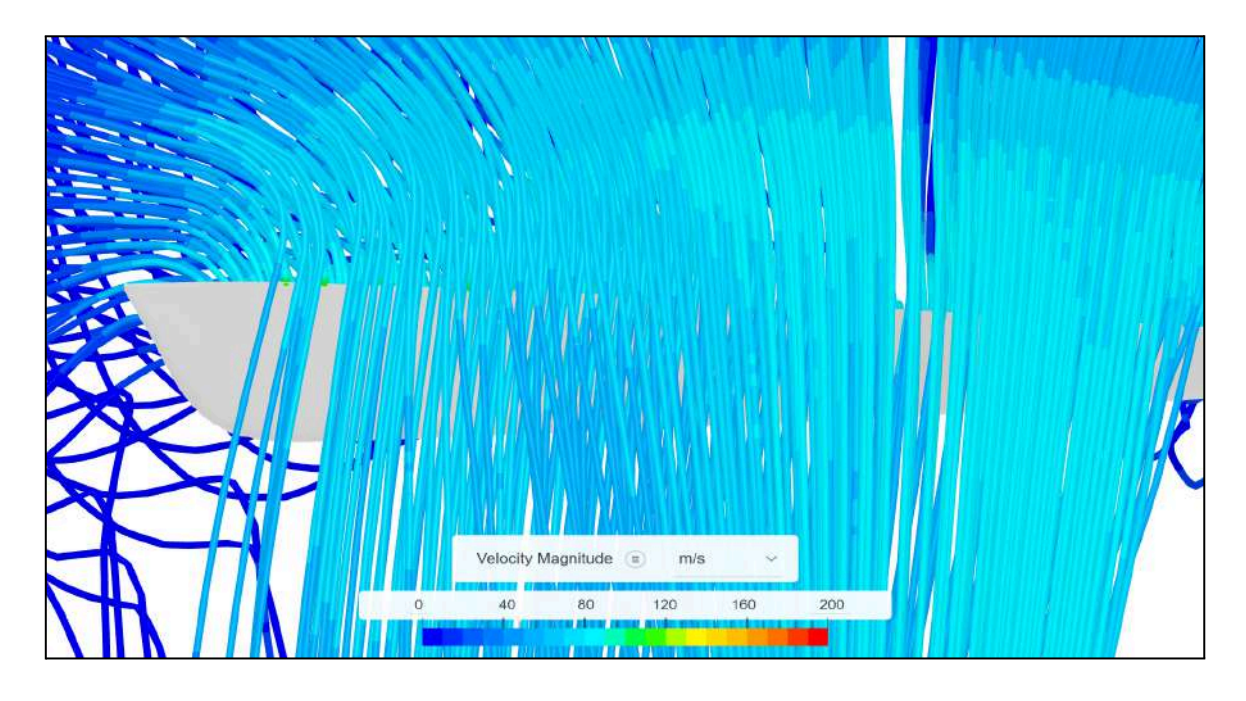


Fig. 6.2.4B Velocity-Colored Airflow Analysis of the **DART** Controlled 25 α Propeller.

6.2.5 Low-Pressure Represented Volumes

Presented are CFD simulation results where the coloring is representative of the low pressure within the illustrated volumes. The CFD simulation platform was provided by our sponsor, SimScale. The comparison is between the fixed-pitch propeller and the DART system with a target of $25\,\alpha$ in an early takeoff scenario.

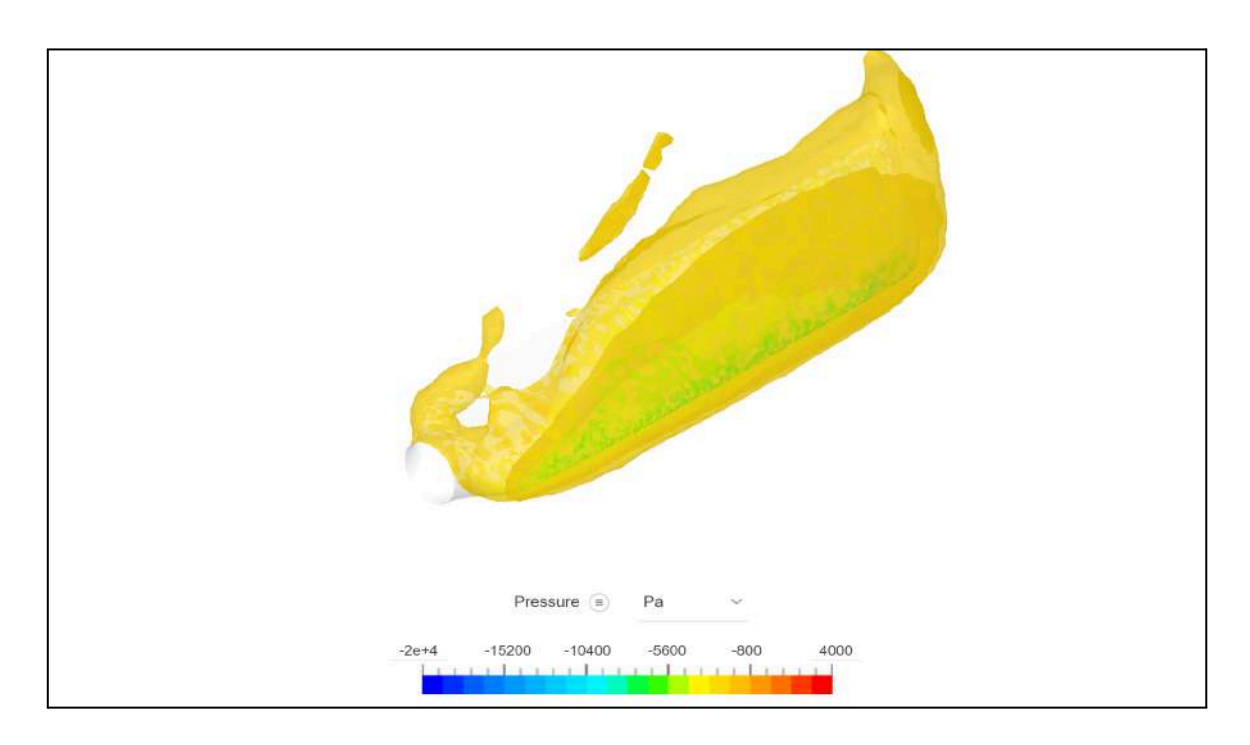


Fig. 6.2.5A Pressure-Colored Volume Analysis of the Cruise-Optimized Fixed-Pitch Propeller.

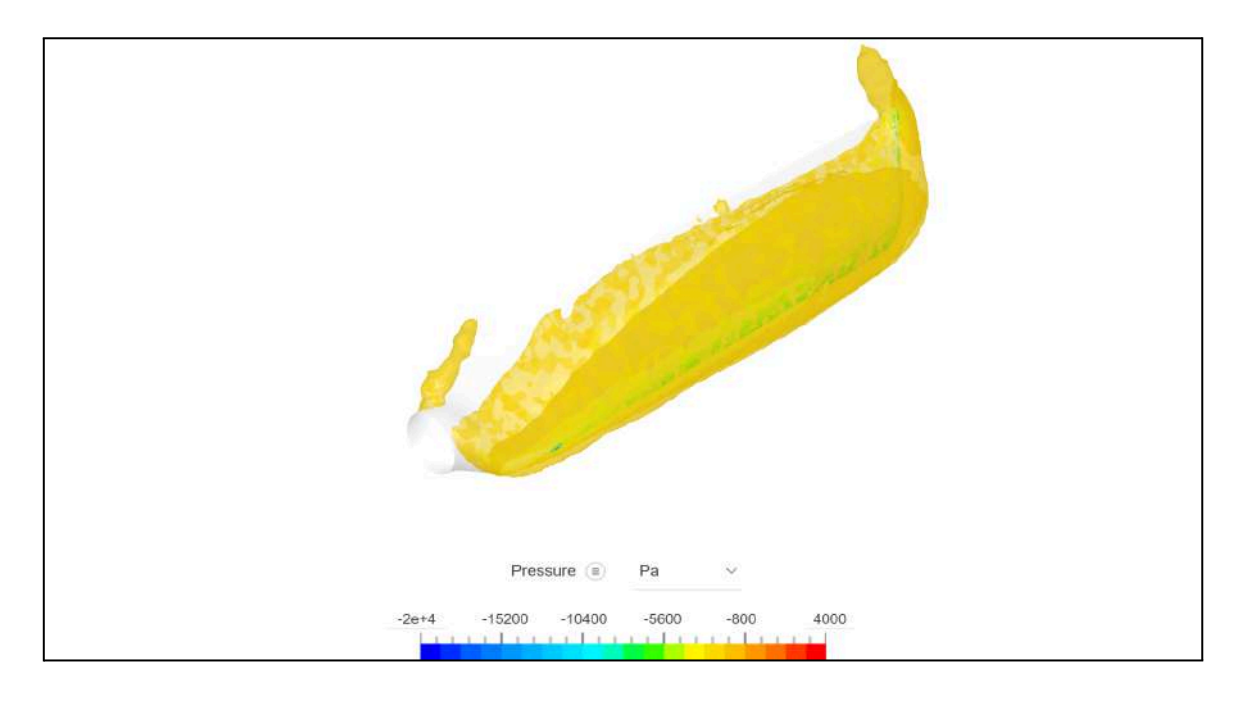


Fig. 6.2.5B Pressure-Colored Volume Analysis of the **DART** Controlled 25 α Propeller.

6.2.6 PACE System Performance

Presented are CFD simulation results where the coloring is representative of the velocity present in the given airflow streams. The CFD simulation platform was provided by our sponsor, SimScale. The comparison is between the fixed-pitch propeller and the DART system with a target of $25\,\alpha$ in a rotation scenario.

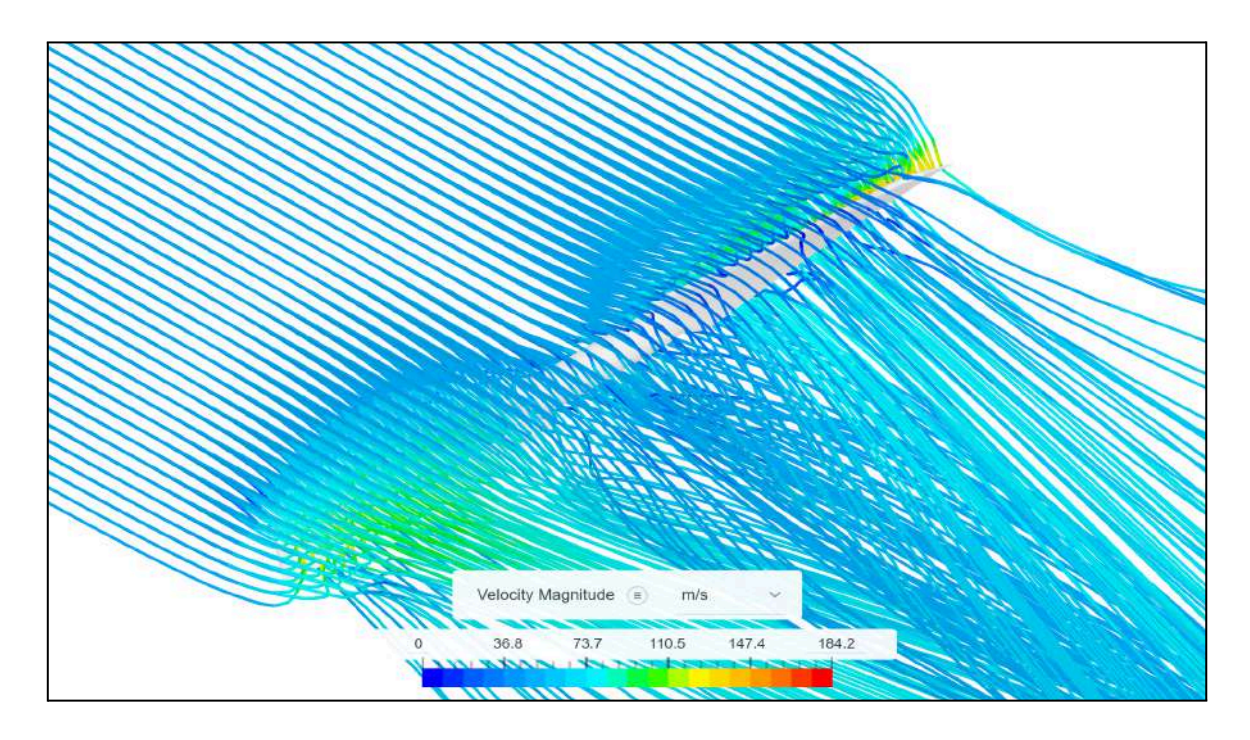


Fig. 6.2.6A Non-PACE Adjusted DART Propeller.

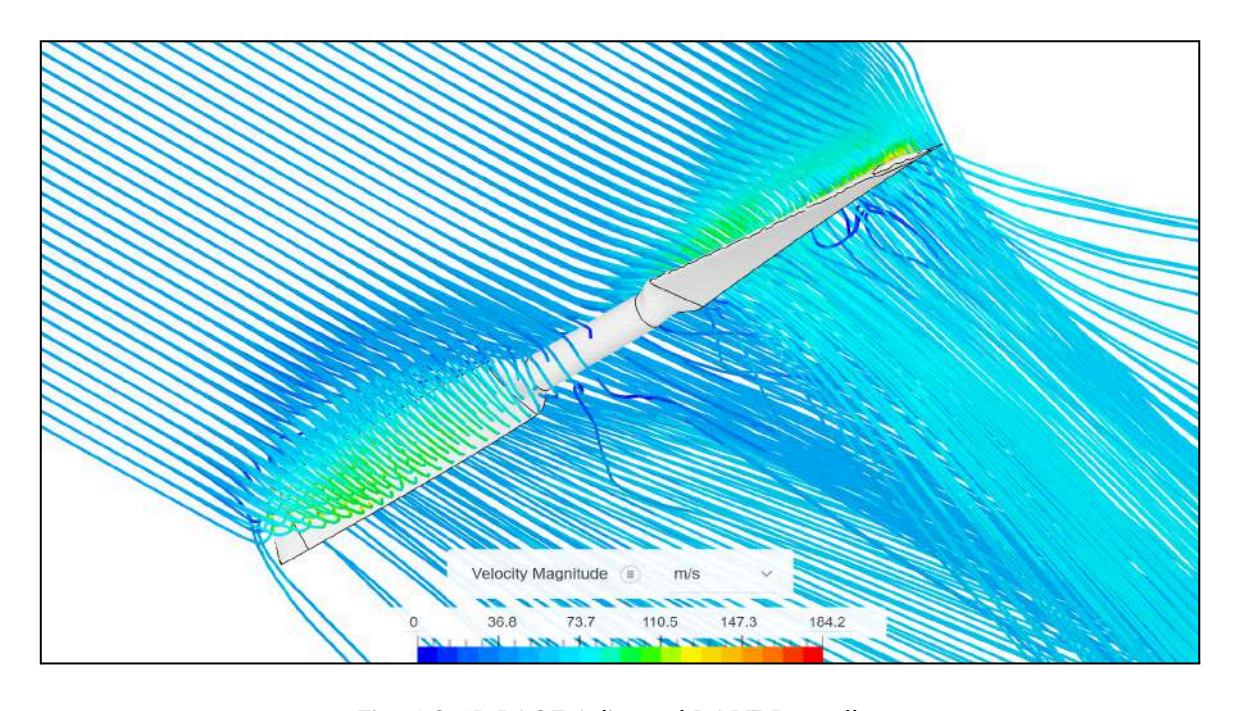


Fig. 6.2.6B PACE Adjusted DART Propeller.

7. Discussion

This section discusses the findings of the research, exploring their significance, limitations, and broader implications in aviation as a whole, alongside an analysis of potential improvements to the project.

7.1 Key Results

Every single scenario tested proved that DART's propeller control provides an **increased thrust-to-drag ratio** compared to the fixed-pitch example. Revised target angle of attack parameters for DART provided **decreased thrust reductions while retaining efficiency**.

DART Takeoff Scenario Compared to a Cruise-Optimized Fixed-Pitch Propeller:

- A thrust reduction of 6,88% resulted in a 31,49%. decrease in aerodynamic drag that
 counteracts the rotation of the propeller, increasing the thrust-to-drag ratio by
 35,92%.
- A thrust reduction of 9,46% resulted in a 47,10%. decrease in aerodynamic drag that
 counteracts the rotation of the propeller, increasing the thrust-to-drag ratio by
 71,15%.
- A thrust reduction of 18,78% resulted in a 59,94%. decrease in aerodynamic drag that counteracts the rotation of the propeller, increasing the thrust-to-drag ratio by 102,77%.
- A significant reduction in overall turbulent flows and TKE was observed, giving way
 to potentially significant noise and vibration reductions, alongside decreased uneven
 aerodynamic loading.
- **Spanwise and chordwise** pressure distribution was observed to have **improved**, with a more evenly distributed low-pressure volume above the propeller blade.

DART Climb Scenario Compared to a Cruise-Optimized Fixed-Pitch Propeller:

 A thrust reduction of 10,38% resulted in a 13,55%. decrease in aerodynamic drag that counteracts the rotation of the propeller, increasing the thrust-to-drag ratio by 3,67%.

General Observations with Regards to Propeller Performance & Efficiency:

- Relying purely on airfoil polar data is not viable for the effective integration of DART, it is highly desirable to run the specific propeller blade through CFD software to establish target angle-of-attacks and to observe the general performance characteristics of the specific blade in various airflows.
- The **Turbulent Kinetic Energy, or TKE,** of the streams in around the propeller are **good indicators** of propeller efficiency. This was concluded through analysing the CFD images and raw thrust and drag data presented above.

7.2 Overall Performance Evaluation

The results are highly indicative of large gains in aerodynamic efficiency with a low impact on thrust. Every single CFD simulation resulted in DART's thrust-to-drag ratio being superior to that of the cruise-optimized fixed-pitch propeller, to varying degrees. However, these ratios, in the takeoff scenario in particular, yielded reduced thrust that in some situations would be impractical and hinder the integration of DART into propeller propulsion systems. After initial DPCS-controlled propeller pitching tests where the angle of attack was governed by mathematical functions, derived from the airfoil polar data detailed in sections 5.4.1 through 5.4.3, CFD-result governed angle of attack targets were established to minimize thrust loss while maintaining significant efficiency gains. The aerodynamic efficiency gains derived from their significant reduction in drag have the potential to increase the range and endurance of electric UAVs and light aircraft due to there being less aerodynamic torque-resistive forces that counteract the propeller's rotation throughout the flight.

The figures displayed in section 6.2.3 present us with striking visuals, illustrating drastic reductions in turbulent airflow and TKE. While a more in-depth aerodynamic analysis is performed in the following section, the reduction in turbulent airflow provides not only aerodynamic efficiency gains, but also probable improvements in acoustics and vibration that can lead to alleviated regulatory hurdles and less mechanical stress on components. Expanding on the issue of mechanical stress, the potential reduction in vibrations paired with the evenly distributed low-pressure volume above the propeller blade illustrated in section 6.2.5, indicates potential improvements in load-distribution across the propeller blade itself, lowering adverse bending moments and component wear.

The simulation run of the PACE system where a non-augmented propeller was compared to a PACE-augmented propeller did not go as planned, indicating no to a slightly negative impact on aerodynamic performance. This did not align with expectations, hence the PACE system being purely theoretical for the time being with future work needed on it. As with the mathematically-modeled performance optimization attempt, the propeller blade has a large and often unexpected effect on the aerodynamic performance, leading to the conclusion of the blade needing to be extensively tested in CFD software to establish its own target angle-of-attacks and operational limits.

A topic that will be discussed in detail in section 7.4 is a revised version of angle of attack targeting. The results showed how the tradeoff between efficiency and thrust can be dynamically controlled. For example, the 59,94% reduction in drag was accompanied by a 18,78% reduction in thrust, while a 31,49% reduction in drag led to a thrust reduction of only 6,88%. These tradeoffs have the potential to be adjusted dynamically to on a per-mission basis, allowing for higher efficiency when a, for example, UAV is operating from a long runway, where maximum thrust is not as imperative.

Overall, DART has exceeded expectations, providing clear and tangible advantages that can be translated into real-world overall and operational efficiency Although the PACE system was not implemented and not proven effective yet, further testing and refinement could help it translate its conceptual nature to that of a working system.

7.3 Aerodynamic Analysis

While numbers are very clear and unambiguous, it is also important to visually assess the airflow and how the propeller blade interacts with it. The illustration also provide additional insight and understanding of aerodynamics, confirming that TKE is in fact a good indicator of propeller performance, among other things.

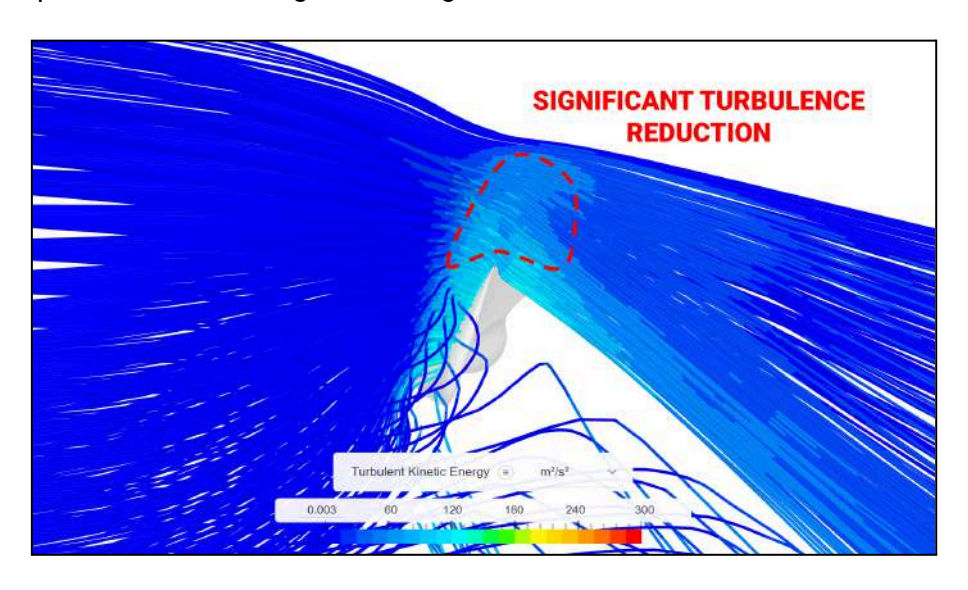


Fig. 7.3A Noted TKE-Colored Airflow Analysis of the **DART** Controlled 25 α Propeller.

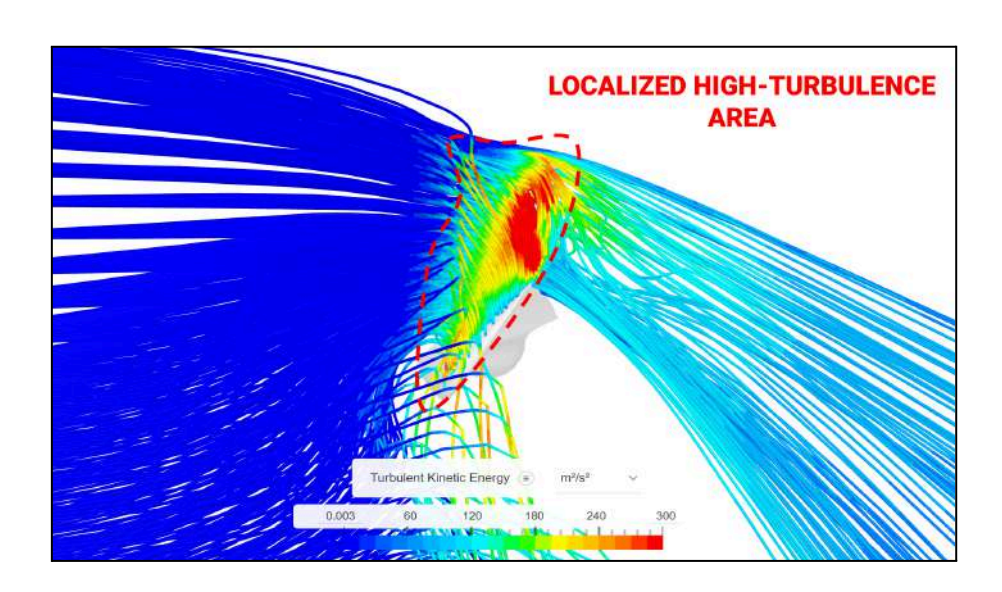


Fig. 7.3B Noted TKE-Colored Airflow Analysis of the Cruise-Optimized Fixed-Pitch Propeller.

As is observed visually and through the data presented in the results section, having DART target, in this case, an angle of attack of the mean chord of 25° results in significantly less disturbances and overall turbulence in the airflow interacting with the propeller. Through both the coloring and a visual assessment of the airflow cylinders, turbulent zones are very pronounced in the fixed-pitch example. It becomes clear that the rapid changes in the airflow's direction yields higher TKE in the affected streams.

It is also worth noting that in Fig. 7.3B the area of turbulence strongly correlates with other aerodynamic experiments and simulations where a large section of turbulence appears above and aft of the airfoil at high angles of attack. The inefficiencies associated with turbulent airflow vectors are even more pronounced when a closer look is taken towards the root and middle section of the fixed-pitch propeller blade example.

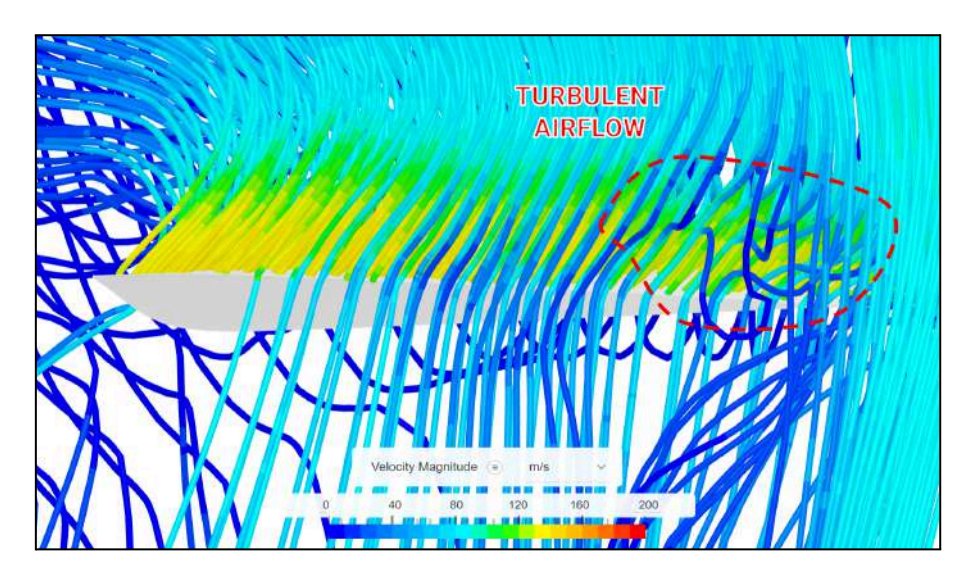


Fig. 7.3C Noted Velocity-Colored Airflow Analysis of the Cruise-Optimized Fixed-Pitch Propeller.

It is problematic that these turbulent airflows occur. This is due in most part to it going against the principles of an airfoil's function, where fast low-pressure air is supposed to travel over the curved top surface to generate a pressure differential that in turn produces a lifting force. However, such issues are not present in DART's case as shown in Fig. 6.2.4B, where the angle of attack is carefully regulated and adapted for the airflow experienced by the propeller at any given time.

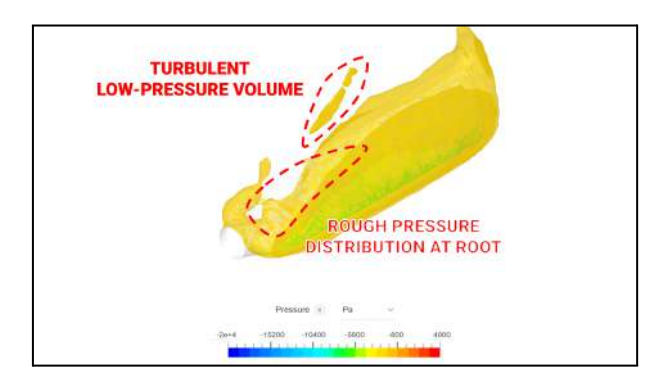


Fig. 7.3D Noted Pressure-Colored Volume Analysis of the Cruise-Optimized Fixed-Pitch Propeller.

Finally, the high TKE combined with the turbulent airflow aft of the propeller blade results in the rough pressure distribution illustrated in the figure above. There is even a detached volume of low-pressure air, likely some sort of wake turbulence. These issues are not present in the DART-controlled system, allowing for the efficiencies detailed in the results section. The reduction in overall turbulent airflows, as stated previously, can also potentially result in less noise and vibrations stemming from the propeller.

7.4 Operational & Systems Integration

It was made obvious early on in the CFD testing of the DART-controlled propeller that purely relies on the mathematical regressions and their corresponding target angle of attack values was simply not practical. While yielding great reductions in torque-resistive drag, they came at the expense of significant thrust loss. However, due to DART's digital system and adaptive nature, this was and will be addressed through simply changing what angle of attack the system should target in any given scenario. Combined with further CFD testing of the specific propeller blade, a lift and drag curve should be able to be drawn on which the systems behaviour is based on.

Furthermore, as illustrated in Fig. 6.2.2B, the degrees to which the propeller is efficient changes in a predictable order. This could be grounds for a subset of the PoF system, where an "efficiency factor" is selected. The function of such an efficiency factor would be to determine how much thrust loss an aircraft can experience given the conditions by which it is operating under in order to be more efficient.

For example, an UAV that is operating from an established airfield with a long runway and good weather might use a high efficiency factor where the 25 α mode is selected, reducing the takeoff thrust by 19% while reducing torque-resistive forces on the propeller by almost 60%. This would lead to less energy spent in the takeoff phase and hence enabling possibly longer range and flight times. On the contrary, if the runway is short or if the atmospheric conditions are adverse, the system might select the 35 α mode where the thrust loss is just 7% while still decreasing drag with 31% to keep the UAV within safe operating margins. It is also worth noting that the thrust loss can be even further reduced. However, this would result in large inefficiencies so this would only be practical in emergency situations.

Such a subsystem described above would be more complex and might require manual pilot input on what efficiency factor to use, somewhat going against DART's fundamental hands-off operating principles. This would not be an issue for UAVs due to their already automated nature, possibly letting ground systems communicate to the UAV about the airport conditions and letting the UAV make a decision for what efficiency factor is best suited. As mentioned previously, this could also lessen regulatory challenges through a reduced atmospheric disturbance. If there is a residential area close to the airfield, it is often in good condition and equipped with a relatively long runway in terms of UAV and light aircraft operation, making a system that increases efficiency while also potentially decreasing acoustic issues be a good fit for more urban missions.

Physically integrating DART into existing and future aircraft comes with some challenges. The mechanism is much larger and more complex than a fixed-pitch configuration, alongside the increased demand for computational power, requiring potential structural revisions and overhaul. However, aircraft equipped with variable-pitch systems and even constant-speed systems already have heavy and complicated mechanisms, making a transition and retrofitting of DART's swashplate design be possibly weight-saving, although as mentioned previously, more computationally demanding.

7.5 Feasibility & Safety

This system was conceptualized, designed, produced, constructed, tested and revised by a teenager in his bedroom, proving that it is feasible from a technical level. A core principle of DART is to utilize existing technologies, a principle which was followed rigorously throughout its development. The issues that can arise from a feasibility perspective is the large-scale implementation of DART, where more advanced materials and reliable actuators are crucial for its safe and efficient operation. It is important to note that the ARC M1 actuators were not intended for end-use cases, being developed for only the DART prototype itself to provide accurate motion control.

On the topic of safety, DART has an autofeather function, immediately actuating the propeller blades to have the least aerodynamic effect on the aircraft in case of an engine failure. This is a common and vital system in propeller aircraft, where the added workload of managing an emergency often leaves room for human operator errors that may or may not result in tragic loss of life. However, the system does not currently have a mechanical fail-safe system for this autofeathering behaviour in the case of a loss in electrical power, leaving room for future developments that would make DART even safer. More robust and fail-safe software would also be needed, where sensor data diagnostics and validation alongside parallel processing of data would be implemented, as found on current modern-day airliners. Systems that would address the over or underspeeding of an electric motor have not been designed yet, but they would be an addition to DART's safety features where using the propeller pitch to affect the motor's rotational speed would only be reserved for urgent or emergency situations due to them going against the operating principles of DART.

7.6 Broader Implications & Significance

In summary, this research and DART has laid the groundwork for a new operational principle of propeller aircraft, being focused on aiding the introduction of electrically-driven light aircraft and UAVs. The results shown above indicate large potential savings in energy while also addressing other operational issues such as noise and vibrations, crucial to overcoming regulatory hurdles.

The comparison naturally yielded less differences between the cruise-optimized fixed-pitch propeller system and the DART propeller system due to the scenarios approaching the cruise phase of the flight. If a fixed-pitch propeller was designed to increase takeoff performance, it would lessen DART's impact in that phase. However, it would enable DART to exceed the fixed-pitch propeller's performance in the often largest phase of flight, being cruise. In the case of variable-pitch systems, DART provides the benefit of real-time hands-off control instead of discrete adjustments at various points throughout a flight, with the configuration automatically alternating between high-thrust and high-efficiency modes depending on the aircraft's situation.

Finally, alongside DART's performance, general correlations between TKE and propeller efficiency were also observed, proving to be good indicators of the forces acting on the propeller blade. The exact degree to which it affects performance and under which conditions needs further research.

7.7 Future Work & Improvements

The improvements to be made are many and very pronounced in certain areas, such as technically implementing the P-factor Augmentation & Control Enhancement, or PACE system. It is important to note that while the prototype moved, the actuators introduced instabilities and jitter, providing even more areas of improvement. Below is a breakdown of the primary issues observed and how they will be addressed:

- Unstable & Jittery Swashplate Motion: This issue lies mainly in the ARC M1 closed-loop actuators used in DART's physical prototype. This will be addressed through a system overhaul and other design changes in the actuator.
- PACE System & Cyclic Pitch Missing: While conceptualized and thought out, there
 were hurdles related to its implementation into the DART software. DPCS had to
 accommodate the use of inverse kinematics to enable cyclic pitch control and with
 the time-constraints that presented themselves at the end of the project, there simply
 wasn't enough time. However, it will be actively worked on to physically realize PACE
 and its cyclic pitch functions, further pronouncing DART's physical capabilities.
- PACE System Revisioning: Alongside the integration issues of PACE, its conceptual foundation was not as stable as thought, providing no to negative impacts on propeller function according to the CFD simulations. More work is needed to both investigate and act upon the airflow the propeller experiences.
- Use of Linear Actuators: While not being mission-critical, for serious and practical
 implementations of DART into an aircraft, it would have to utilize linear instead of
 rotary actuators due to the spatial constraints. This will not be actively worked on for
 now, but it might be looked into at a later date.
- Operational Testing: There is an idea to try implementing the control logic of DART into a flight simulator where a user can interact with the propeller aircraft and it would act accordingly, reading parameters and adjusting the propeller blades dynamically. This would have a substantially positive impact on DART's development, enabling more realistic testing and fast-paced iterative development.
- Mechanically-Backed Autofeather System: As mentioned previously, a mechanical
 fail-safe autofeather system would prove beneficial to implement and allow for
 further integration into larger aircraft. If electrical power is lost, the independent
 mechanical system, such as the ones found on many propeller aircraft, would enable
 the feathering of the propeller system regardless of external factors.
- More Robust & Fail-Safe Computer Systems: More advanced systems need to be implemented to allow for a fail-safe architecture, aligning with the safety-oritented core of the aviation industry as a whole. Features such as data-validation and parallel processing of information needs to be present for the integration of this system onto larger aircraft.

8. Conclusion

In conclusion, the DART system introduces real-time adaptive propeller control, aimed at electric aircraft in particular, that demonstrates large efficiency gains compared to conventional propeller systems. In addition to aircraft-bound efficiences, there is also potential for noise and vibration reductions, aiding in regulatory challenges and mechanical wear and tear.

The DART system focuses on reducing the torque-resistive aerodynamic drag of the propeller, reducing the force required to continually spin the propeller throughout a flight. This fundamental shift in operating principles was proven effective through computational fluid dynamics simulations, significantly reducing the torque-resistive drag of the propeller blades at the expense of only slight thrust reductions. This brought the favourable thrust-to-drag ratios that defined the efficiency of DART, being between 35% and 102% more efficient, depending on DART's configuration, than a cruise-optimized fixed-pitch propeller system in a takeoff scenario. These numbers were in large parts results of the lowered turbulent kinetic energy present in air streams and improved pressure distribution across the propeller blade.

The physical realization of DART is a combination of hardware and software. The paper report details their developments and their iterative design process enabled by the extensive use of fused-deposition modeling additive manufacturing technology. The software is designed to react to emulated sensor data, provided by a user interface where flight and control parameters such as airspeed, pressure, temperature, and landing gear status can be augmented at any time, demonstrating DART's real-time capabilities. After assembling the prototype, it reacted instantly to changes in emulated sensor data as they were happening, proving the technical feasibility of DART.

The software ended up consisting of three systems, although four were planned. Each system is its own program with its own inputs and outputs, enabling them to work together to achieve automated propeller pitch control that can alternate between high-thrust and high-efficiency modes, continuously adapting the propeller's power output to the performance requirements of the aircraft throughout the flight. Alongside normal propeller control, DART has built-in safety features, such as digital reverse-thrust inhibition and autofeathering capabilities, staying grounded to its roots in aviation where safety is paramount. There were plans to implement the fourth system that would counteract asymmetric thrust forces, however, due to time and technical constraints, it was not physically realized and will need further research.

Finally, this paper serves as documentation of the journey I, the author, took to create the Digital Airflow-Reacting Tuning propeller system. There were many challenges and hurdles along the way, from design through to integration. However, the system proved to be effective and a stepping stone towards future developments, holding promise for electric propeller propulsion technology in light aircraft and UAVs, contributing to a more sustainable form of aviation.

9. References

biswayandutta2000. (2024). Electric motors vs combustion engines: RPM showdown. *Techtales*. https://techtales.co.in/electric-motors-vs-combustion-engines-rpm-showdown/

Constant Speed Propeller. (n.d.) *SKYbrary Aviation Safety*. https://skybrary.aero/articles/constant-speed-propeller

Variable Speed Propeller. (n.d.) *SKYbrary Aviation Safety*. https://skybrary.aero/articles/variable-pitch-propeller

Thijssen, R., Proesmans, P., & Vos, R. (2022). Propeller Aircraft Design Optimization for Climate Impact Reduction. In *ICAS PROCEEDINGS 33th Congress of the International Council of the Aeronautical Sciences* Article ICAS2022_0819 International Council of the Aeronautical Science (ICAS).

https://www.icas.org/ICAS_ARCHIVE/ICAS2022/data/papers/ICAS2022_0819_paper.pdf

Unmanned Aerial Vehicle (UAV) Drones Market Size Expected to Reach USD 169.7 Bn by 2033. (2024). *GlobeNewsWire*.

https://www.globenewswire.com/news-release/2024/08/09/2927741/0/en/Unmanned-Aerial-Vehicle-UAV-Drones-Market-Size-Expected-to-Reach-USD-169-7-Bn-by-2033.html

Full Authority Digital Engine Control. (n.d.) *SKYbrary Aviation Safety*. https://skybrary.aero/articles/full-authority-digital-engine-control-fadec

Coefficient of Determination. (n.d.) Newcastle University.

https://www.ncl.ac.uk/webtemplate/ask-assets/external/maths-resources/statistics/regression-and-correlation/coefficient-of-determination-r-squared.html

Raspberry Pi Ltd. (2024). Raspberry Pi Pico 2 Datasheet [PDF]. https://datasheets.raspberrypi.com/pico/pico-2-datasheet.pdf

ams. (2020). AS5600 [PDF].

https://files.seeedstudio.com/wiki/Grove-12-bit-Magnetic-Rotary-Position-Sensor-AS5600/res/Magnetic%20Rotary%20Position%20Sensor%20AS5600%20Datasheet.pdf

STEPPERONLINE. (n.d.). NEMA 11 Bipolar Stepper Motor Website Page. STEPPERONLINE. https://www.omc-stepperonline.com/nema-11-bipolar-1-8deg-12ncm-17oz-in-0-67a-6-2v-28x28x51mm-4-wires-11hs20-0674s?srsltid=AfmBOooVhD3hUHERjpdQ3xpMyYgalcqR5E5GiwWrCtVsW-NPdtCzM7AJ

Analog Devices. (2023). TMC2202, TMC2208, TMC2224 Datasheet. [PDF]. https://www.analog.com/media/en/technical-documentation/data-sheets/TMC2202_TMC2208_TMC2224_datasheet_rev1.14.pdf

Market Snapshot: Battery electric vehicles are far more fuel efficient than vehicles with internal combustion engines. (2021). Canada Energy Regulator.

https://www.cer-rec.gc.ca/en/data-analysis/energy-markets/market-snapshots/2021/marke

 $\frac{t\text{-}snapshot\text{-}battery\text{-}electric\text{-}vehicles\text{-}are\text{-}far\text{-}more\text{-}fuel\text{-}efficient\text{-}than\text{-}vehicles\text{-}with\text{-}internal\text{-}co}{mbustion\text{-}engines\text{.}html}$

Kosourova, E. (2024, December 11). What is Python Used For? 8 Real-life Python Uses. Datacamp.

https://www.datacamp.com/blog/what-is-python-used-for